Brüel & Kjær

Technical Review

To Advance Techniques in Acoustical, Electrical, and Mechanical Measurement

ANALOG EXPERIMENTS COMPARE IMPROVED SWEEP RANDOM TEST WITH WIDE BAND RANDOM AND SWEEP SINE TESTS

No 3 1965

PREVIOUSLY ISSUED NUMBERS OF BRÜEL & KJÆR TECHNICAL REVIEW

1-1960 Pressure Equalization of Condenser Microphones and Performance at Varying Altitudes.

2-1960 Aerodynamically Induced Noise of Michrophones and Windscreens.

3-1960 Vibration Exciter Characteristics.

4-1960 R.M.S. Recording of Narrow Band Noise with the Level Recorder Type 2305.

1-1961 Effective Averaging Time of the Level Recorder Type 2305.

2-1961 The Application and Generation of Audio Frequency Random Noise.

3-1961 On the Standardisation of Surface Roughness.

4-1961 Artificial Ears for the Calibration of Earphones of the External Type.

1-1962 Artificial Ears for the Calibration of Earphones of the External Type, part 2.

2-1962 Loudness Evaluation.

3-1962 Testing of Stereophonic Pick-ups by means of Gliding Frequency Records.

4-1962 On the Use of Warble Tone and Random Noise for Acoustic Measurement Purposes.
Problems in Feedback Control of Narrow Band Random Noise.

1-1963 Miniature Pressure Microphones.
Methods of Checking the RMS Properties of RMS Instruments.

2-1963 Quality Control by Noise Analysis.
A. F. Nonlinear Distortion Measurement by Wide Band Noise.

3-1963 Effects of Spectrum Non-linearities upon the Peak Distribution of Random Signals.

4-1963 Non-linear Amplitude Distortion in Vibrating Systems.

1-1964 Statistical Analysis of Sound Levels.

2-1964 Design and Use of a small Noise Test Chamber.
Sweep Random Vibration.

3-1964 Random Vibration of some Non-Linear Systems.

4-1964 The Accuracy of Condenser Michrophone Calibration Methods. Part I.

1-1965 The Accuracy of Condenser Microphone Calibration Methods. Part II.

2-1965 Direct Digital Computing of Acoustical Data.
The Use of Comparison Bridges in Coil Testing.

TECHNICAL REVIEW

No. 3 - 1965

Contents

K. LARSEN & SØN - LYNGBY

Analog Experiments Compare Improved Sweep Random Tests with Wide Band Random and Sweep Sine Tests*)

By

Galt B. Booth
MB Electronics,
New Haven, Connecticut

Jens T. Broch
Brüel & Kjær
Nærum, Denmark

ABSTRACT

After a brief review of the "historical" background of sweep random vibrating testing an experimental study is described in which the electrical analog of a resonant mechanical device on a vibration exciter was subjected to a number of carefully controlled vibration tests. These tests included the common wide band random test, the sweep sine test, and a variety of different sweep random tests with differing system time constants.

The responses of this resonant system to the various tests were carefully measured in a standardized manner and plotted in a common form so that the results of the different vibration test techniques may be directly compared.

The results of the experiments are used to develop accelerated sweep random tests. A new sweep random test technique is proposed which better takes into consideration the time available for testing.

SOMMAIRE

Après un court historique de la technique des essais aux vibrations aléatoires sous une bande glissante, on décrit une étude expérimentale dans laquelle l'analogue électrique d'un dispositif mécanique résonnant sur un excitateur de vibrations fut soumis à un certain nombre d'essais aux vibrations, soigneusement contrôlés. Ils comprenaient l'essai habituel sous large bande, l'essai sous une sinusoïde balayée et une variété d'essais différents aux signaux aléatoires balayés, avec des constantes de temps de système différentes.

Les réponses de ce système résonnant à ces divers essais, furent soigneusement mesurées d'une manière uniformisée, et consignées de manière que les résultats des différentes techniques d'essai aux vibrations puissent être directement comparées.

Les résultats des expériences sont utilisés pour établir les formes d'essais accélérés sous signaux aléatoires balayés. Une nouvelle technique d'essai sous signaux aléatoires balayés est proposée qui tient mieux compte du temps disponible pour l'essai.

ZUSAMMENFASSUNG

Schmalbandrauschen gleitender Frequenz findet seit einiger Zeit Anwendung in der mechanischen Prüftechnik zur Steuerung von Schwingerreger-Anlagen, wobei die Zuverlässigkeit eines Prüflings unter dem Einfluß mechanischer Schwingungen untersucht wird. Andere Prüfverfahren arbeiten mit Sinus oder mit Breitbandrauschen.

Die folgende Studie vergleicht die Wirkung der drei genannten Signalformen an Hand eines Experiments. Eine elektrische Ersatzschaltung übernimmt hierbei die Rolle des mitschwingenden Prüflings. Aus den Versuchsergebnissen läßt sich ein abgekürztes Prüfverfahren für Schmalbandrauschen ableiten, welches die verfügbare Prüfzeit besser berücksichtigt.

---

*) Paper presented at the 34th Symposium on Shock, Vibration and Associated Environments, Monterey, California on October 15, 1964.

History.

Although the wide band random test is generally accepted, it is costly and a less costly substitute has been sought ever since its first introduction. Various "equivalent" sweep sine tests have been proposed but since the sweep sine test cannot produce the same distribution of acceleration and stress amplitudes within the test specimen no general equivalence between the two types of test is ever likely to be found. In 1957, M. W. Olesen of the Naval Research Laboratory proposed a sweeping narrow band random vibration test, a test which actually constitutes a compromise between a wideband random vibration test and a sweep sine test. It operates on the principle of replacing the low acceleration density wideband random excitation with an intense, narrow-band random excitation sweeping slowly over the frequency range of the test. In 1960, G. B. Booth showed how to calculate the acceleration level and the test time needed to make a sweep random test correspond to a wideband test. It was shown that the sweep random test can produce the same number of important stresses and accelerations, at each level, as the wide band test. For a long time the equipment necessary to perform this kind of testing was not commercially available, and very little progress was made in the use of the method. Recently, the complete control equipment required for sweep random vibration testing has been developed in the form of two units: a Sine-Random Generator, and a Vibration Meter. Also considerable efforts have been, and are being made to evaluate and extend the test. The more theoretical parts of the work are being confirmed by means of tests on electro-mechanical models while a number of comparative damage studies are currently in the planning and preliminary test stages.

Objectives.

The program reported in this paper has four objectives:

- To experimentally confirm the theoretical calculations* of the distribution of response accelerations to a sweep random test,
- To experimentally determine other response acceleration distributions obtainable with the control equipment,
- To develop time-level exchange curves useful in the shortening of sweep-random test times, and
- To propose an improved sweep random test procedure.

Technique.

The block diagram, Figure 1, shows the equipment used to perform the sweep random test. The narrow band random acceleration excitation to the test specimen is monitored by an accelerometer, read on a meter, and applied to a compressor circuit which controls the gain of a variable gain stage. The level of a narrow band random voltage of sweeping center frequency is controlled by this variable gain stage. The power amplifier then amplifies this

---

*) Refer to Appendix A for a derivation of the sweep random test.

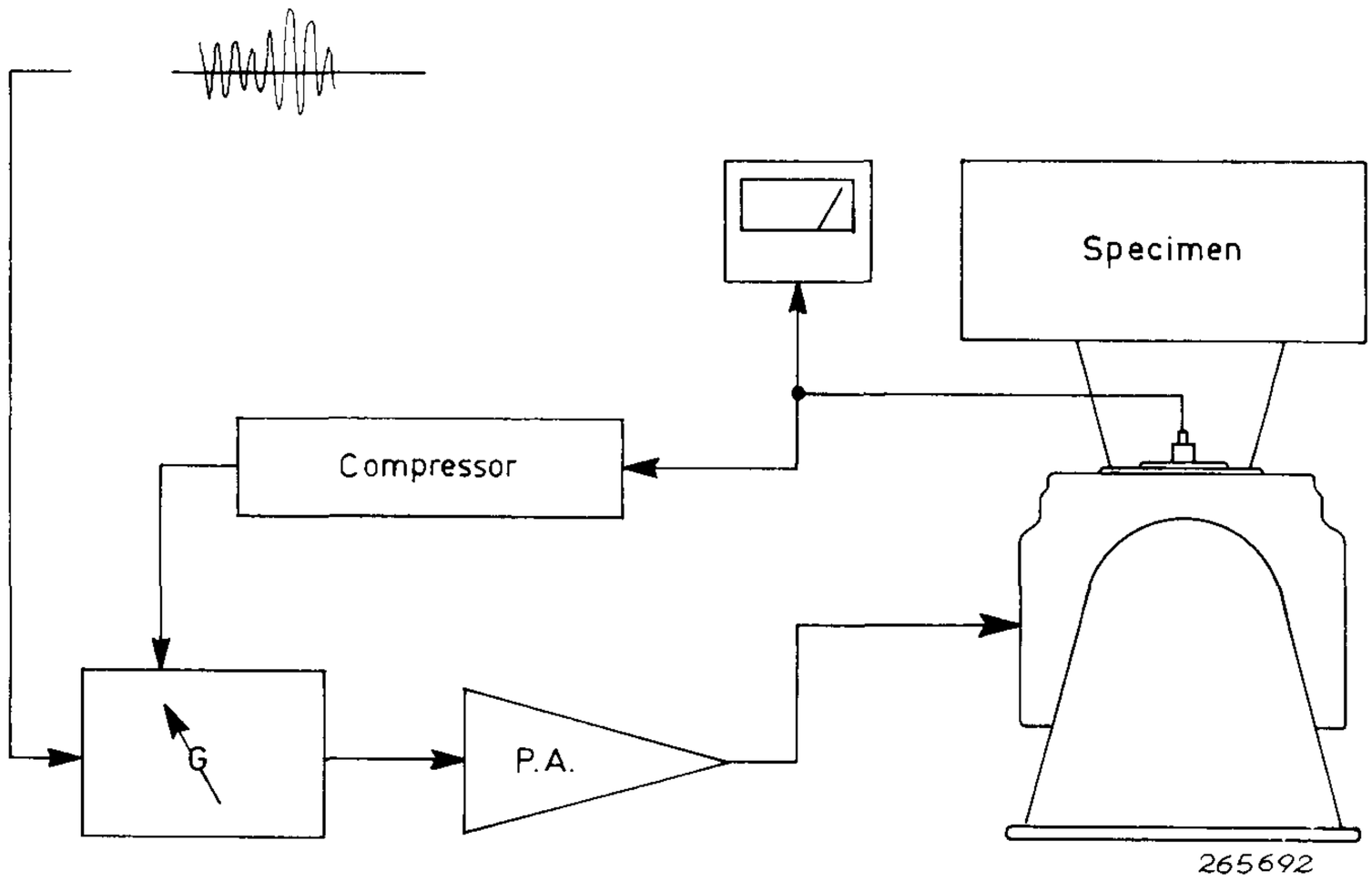

Fig. 1. Block diagram showing operation of equipment to perform the sweep random test.

sweeping narrow band random voltage to a power level adequate to drive the vibration exciter and specimen.

To study the distribution of response acceleration peaks, an electrical analog of a mechanical specimen was built. Figure 2a shows the mechanical block diagram of any normal vibration mode of the test specimen. a_t is the acceleration of the vibration table and a_s is the response acceleration of the mass. The ratio, a_t/a_s, of the response acceleration to the table acceleration is shown by the curve to the right.

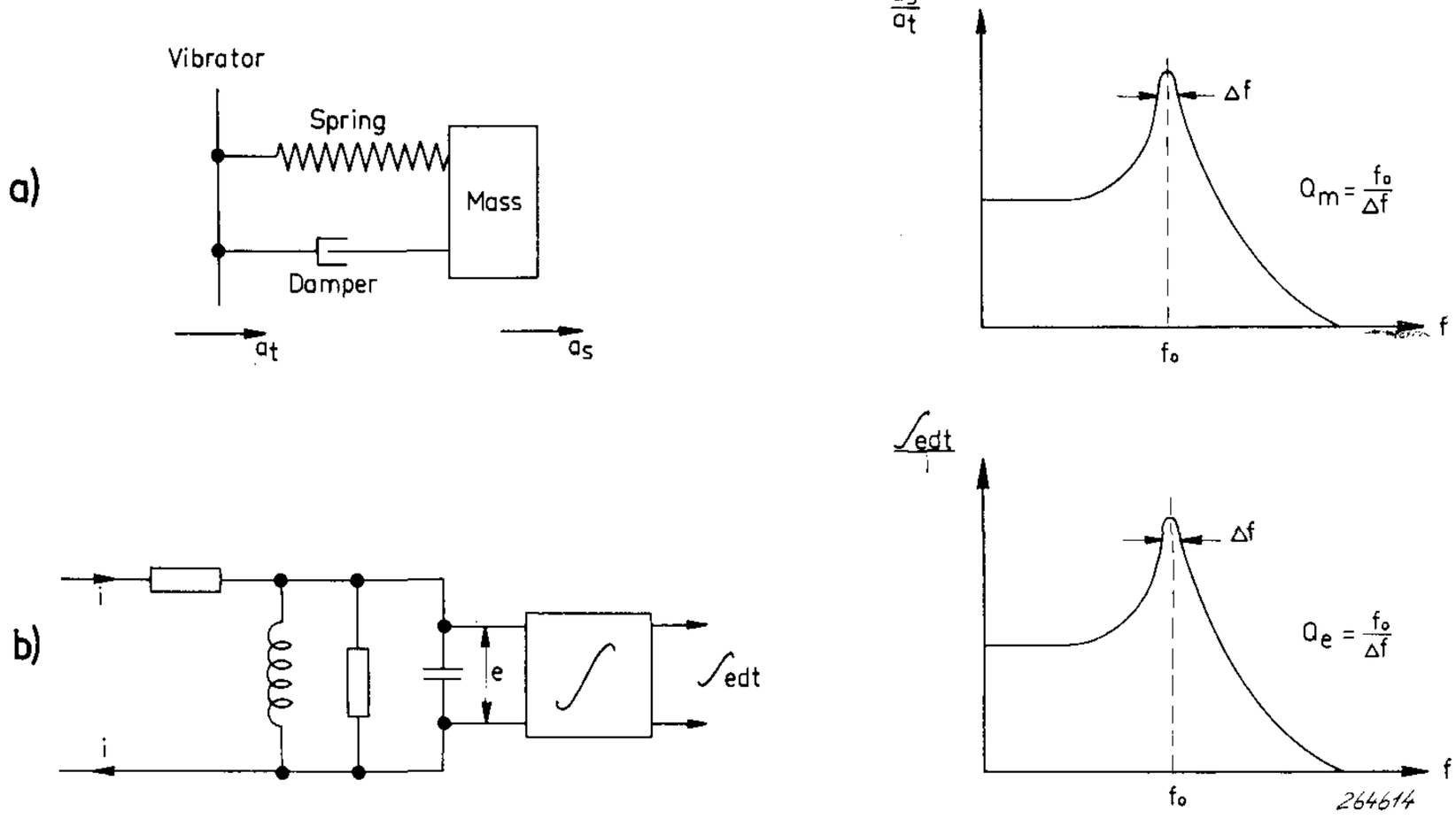

Fig. 2. Analog of Mechanical Normal Vibration Mode. a) Mechanical schematic and ratio of response to input accelerations. b) Electrical analog and ratio of integrated capacitor voltage to input current.

The electrical analog shown in Figure 2b was chosen for experimental convenience. The input current, i, is made proportional to the vibrator table acceleration, a_t. The integral of the voltage across the capacitor is then proportional to the mass acceleration, a_s. The diagram to the right shows that the ratio of the integrated capacitor voltage to the input current has the same form as the response of the mechanical system.
The diagram of Figure 3 shows the control equipment, the analog, and the measuring instrumentation. The circuit was fed from the Sine-Random Generator set to produce a constant acceleration gradient*) by means of the

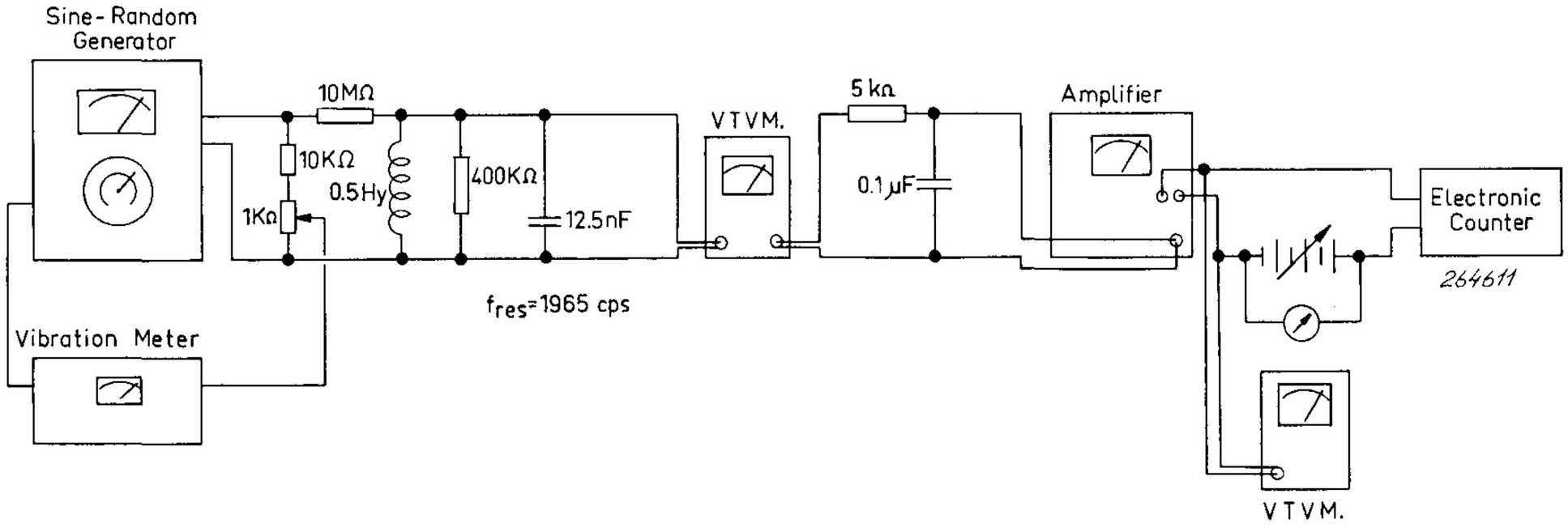

Fig. 3. Schematic showing control equipment, the analog, and the measuring instrumentation.

fedback through the Vibration Meter. To keep the current independent of the impedance of the test circuit, a 10 Megohm isolation resistor was used. The circuit was tuned to 1965 cps and adjusted to a Q of 20.2 by means of a damping resistor. To measure an output proportional to the acceleration of the mass the output voltage from the circuit was isolated from the test circuit by means of an amplifier having a high input impedance (10 Megohms). Finally the output of a second isolation amplifier was fed to a counting arrangement. A special random noise voltmeter, having a wide selection of integration time constants and an rms rectifier, was used to measure the rms value of the output signal.
A counting arrangement was used to count the number of times the signal crossed a reference level, b, with positive slope, Figure 4. The level was set by means of the battery and was adjusted to the following multiples of the rms response level: o.5, 1.0, 1.5, 2.0, 2.5, 3.0, 3.5. The rms value was arbitrarily chosen to be 8 volts which made the variation in the counter firing level, some .2 volts, negligible. A further inaccuracy is due to the difficulty in setting the DC voltage exactly to the correct multiple of the rms value. This is most critical at high multiples of the rms value, because of the steepness of the slope of the measured curve, Figures 6 through 8. It was found that this error was about $\pm$ o.1 volt. Furthermore, the resulting counts are

*) See Appendix A.

subject to the usual statistical errors related to the sample sizes, however, these statistical errors are small except at 3.5 times the rms response level where the counts come in clumps.

Measurements.
A number of tests were made, keeping the level b in Figure 4 fixed, and sweeping the narrow band of noise back and forth through the resonance of the analog, counting the number of level crossings.

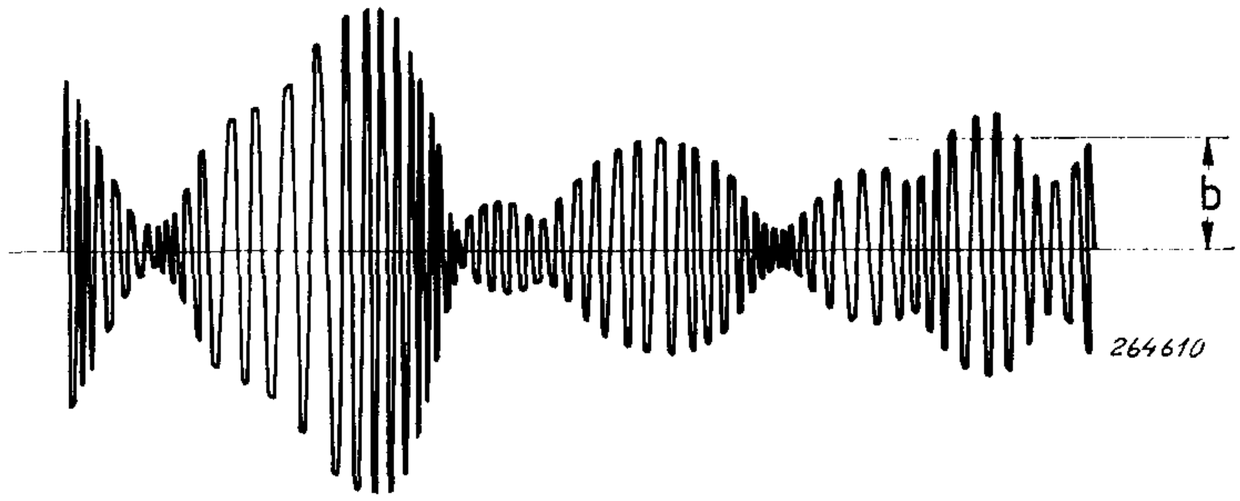

Fig. 4. Narrow band random acceleration signal and reference acceleration level, b. Counts made of number of peaks exceeding b.

By changing the level, b, and repeating the experiments for various settings of the sweeping bandwidth and compressor speed the set of curves shown in Figure 5 were plotted. The various curves are marked with a figure, β, defined as the ratio between the compressor speed and the test noise bandwidth. The ratio, β, is significant because only the interaction between the fluctuations of the noise envelope and the regulation speed changes the distribution of vibration excitation peaks significantly.
The ordinate of the curves is the ratio of the number, N_b, of peaks exceeding the level, b, to the total number of peaks occurring in a sweep over the —3 dB bandwidth of the analog circuit. Although during the experiments the frequency was varied between the —10 dB points of the circuit resonance curve, most of the vibrational energy imparted to the specimen during test is between the —3 dB frequencies.
It can be seen from the curves that no change in the peak distribution occurs for β lower than 33 which means that for these values of β no interaction takes place between the fluctuations of the noise envelope and the automatic level regulation. The results obtained for these low β values can also be verified theoretically, see Appendix A, and the curve Figure 6a).
Finally, for the sake of comparison, the peak distribution obtained by sweeping a sine-wave through the resonance is also shown in Figure 5. It should be noted that a certain upper limit in peak level here exists, 1.42, and that the shape of the distribution is considerably different from those obtained with a fluctuating signal. Also, when sweeping with a sine-wave the peak build-up repeats itself each sweep, which is significantly different when fatigue damage accumulation is considered.

Peak Distribution Matching.

To obtain an equivalence between a wideband random test and a sweep random test it is important that the distribution of acceleration response peaks at the higher response levels be similar. It is well known that the distribution of response peaks of a lightly damped single degree-of-freedom system follows the Rayleigh distribution when the system is excited by wide band Gaussian noise. Since the integral of the Rayleigh distribution, shown in Figure 6b), is known, it was used to confirm the operation of the instrumentation.

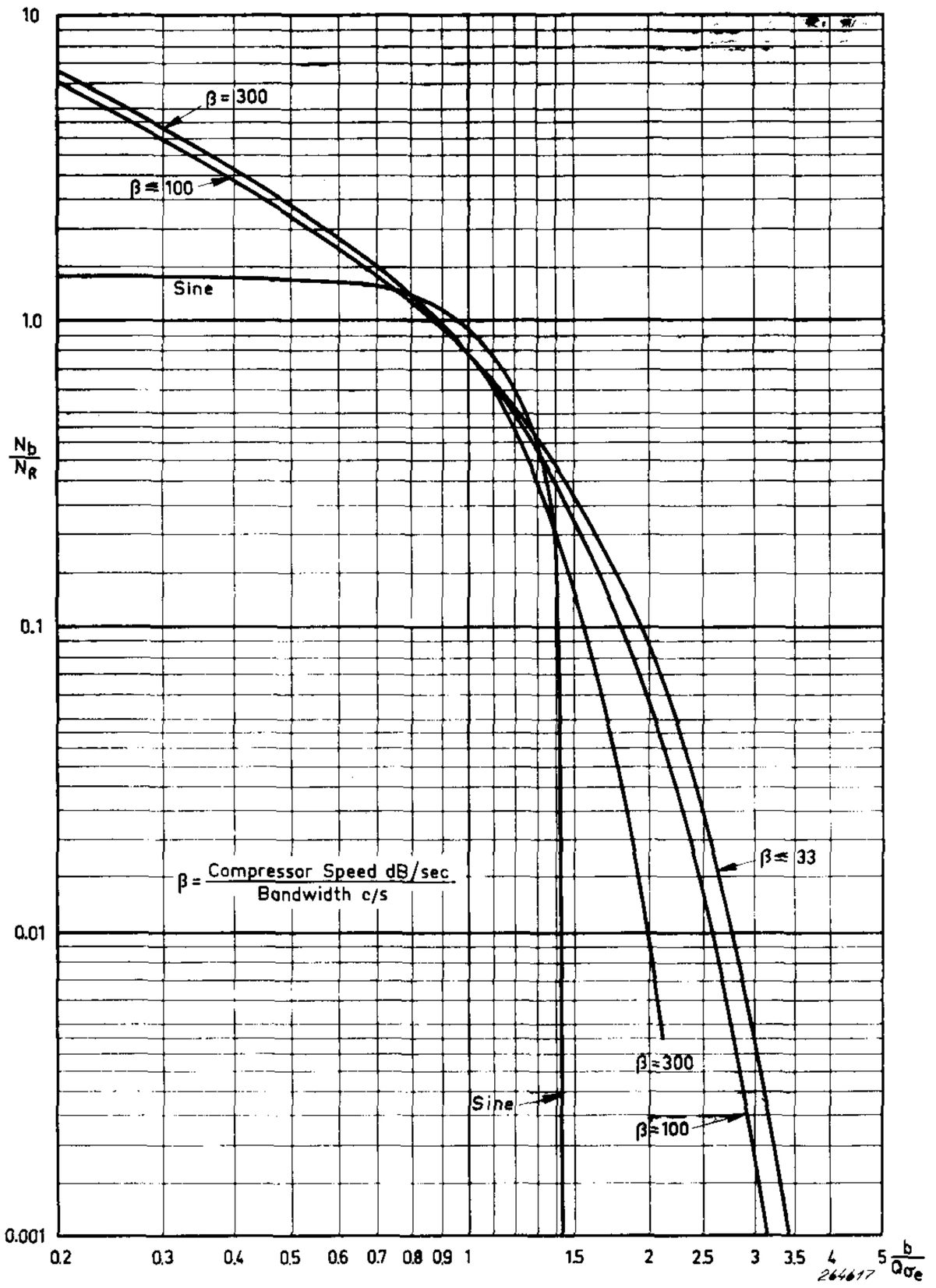

Fig. 5. The ratio of the number of peaks exceeding the level b to the total number of cycles in the resonance bandwidth for sweep random tests with various compressor speeds and for the sweep sine test.

To match a sweep random test to a wide-band test, the distribution curves shown in Figure 5 must be matched to the integrated Rayleigh curve. In Figure 7 an example of the matching technique is shown. As all of the curves shown are plotted to logarithmic scales, a "sliding" of the axis by the amounts

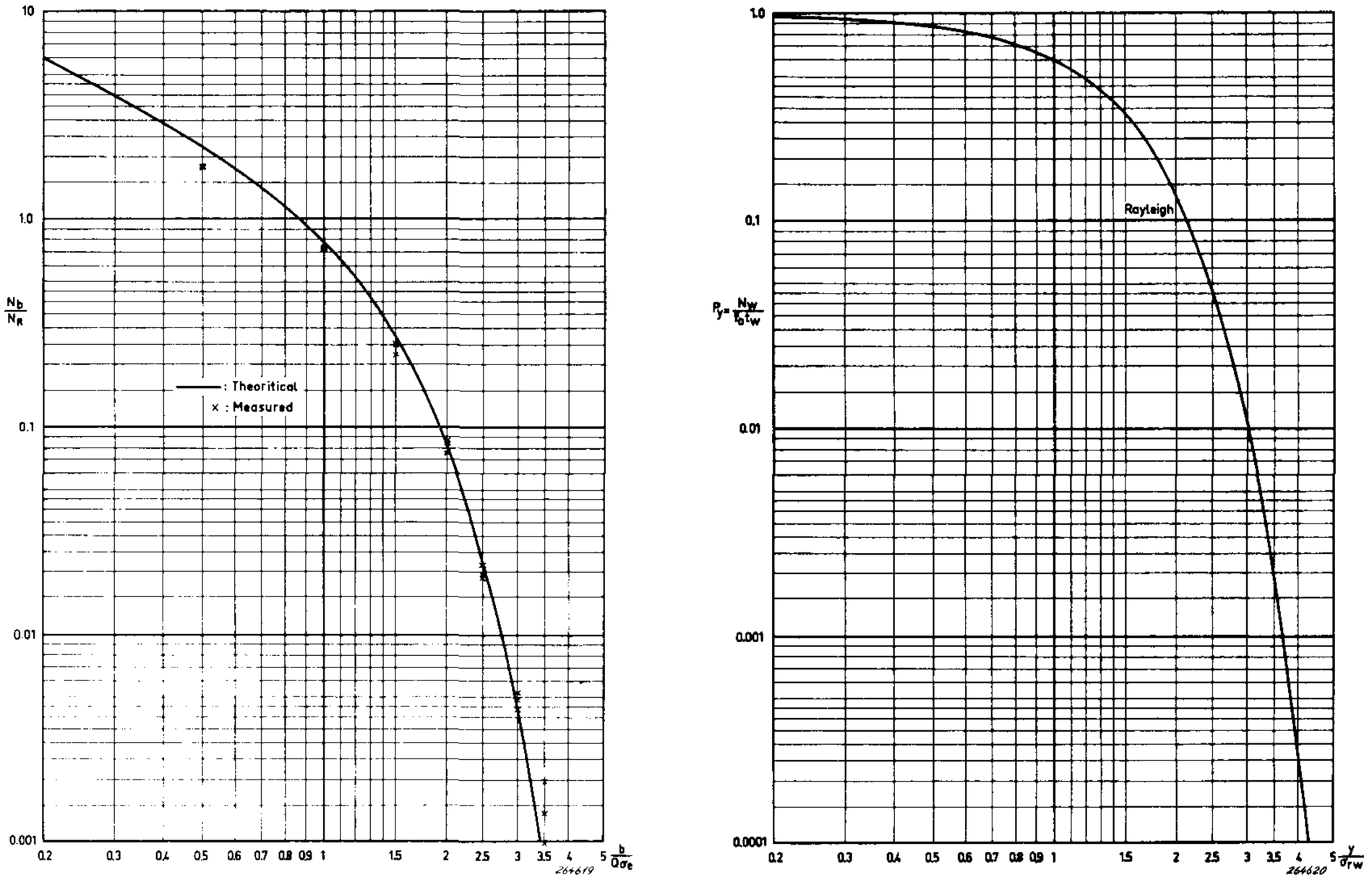

a) *b)*

Fig. 6a) Comparison of theoretical and experimental distributions of acceleration peaks for slow sweep random test. b) Integral of Rayleigh amplitude distribution, showing the ratio of the number of acceleration peaks exceeding the level y to the total number of response acceleration peaks for the wide band random test.

q and s, see Figure 7, actually means a multiplication of the quantities involved, as with a slide-rule. Thus, looking at the x-axis (abscissae), the rms level of the sweep random test is multiplied by the factor q to provide the best possible peak matching.
The test level of the sweep random equivalence is:*)

$$\gamma = q \sqrt{\frac{G}{80}}$$

Similarly, the test time for the sweep represented by the ordinates in Figure 7 must be multiplied by the factor s:*)

$$t_n = s \times 20\, t_w \ln \frac{f_H}{f_L}$$

In these formulae, γ is acceleration gradient ($g\sqrt{sec}$), G is acceleration spectral density (g^2/cps), t_n is test time for the sweep random test (min.), t_w is test time for the wide band test (min.), f_H is upper limit of the frequency sweep, and f_L is lower limit of the frequency sweep.

---

*) See Appendix A.

To set up a sweep random test which complies with the wide band specifications

$G = 0.2\ g^2/cps$ from 20 cps to 2000 cps, and

$t_w = 2$ minutes;

if the matching shown in Figure 8 were used, the acceleration gradient would be

$$\gamma = 0.058\ g\sqrt{sec}$$

and

$$t_n = 156 \text{ minutes}$$

This test time may be considered too long. It is possible to reduce this time, while retaining a good distribution of acceleration response peaks, by the technique described in the next section.

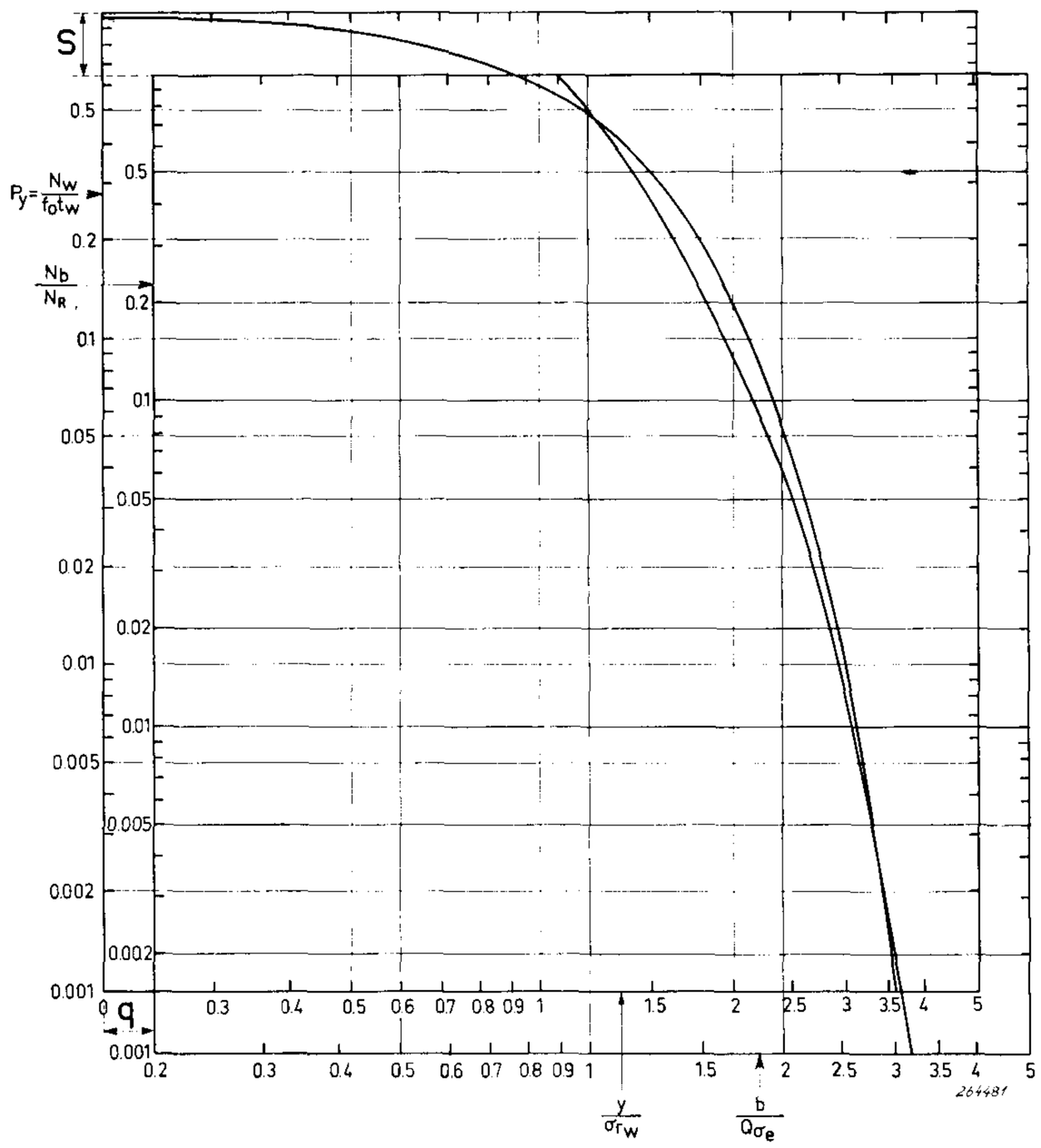

Fig. 7. Matching of sweep random response acceleration peak distribution to wide band random response acceleration peak distribution showing test time factor, s, and the level factor, q.

Accelerated Testing.

As an objective, accelerated testing should reduce the duration of the sweep random test, while keeping the number of response acceleration peaks at each level the same as the wide band test.

Since the curves of Figure 5 have differing shapes for the various β values, it is possible to match the curves to the integrated Rayleigh curve of Figure 6b) in many ways. Figures 8a, 8b, and 8c illustrate three of the more useful matching situations. In each case the sweep random curve was placed to give

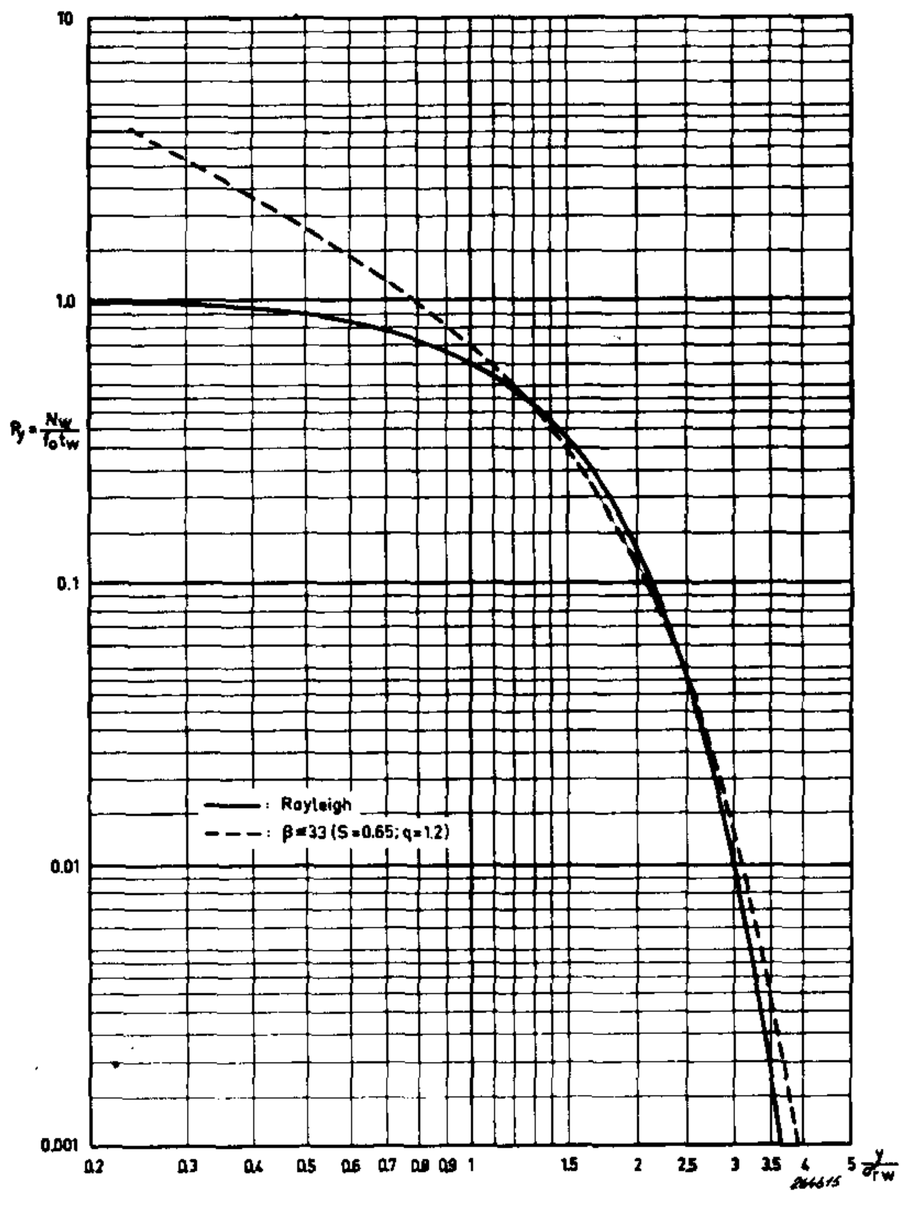

a)

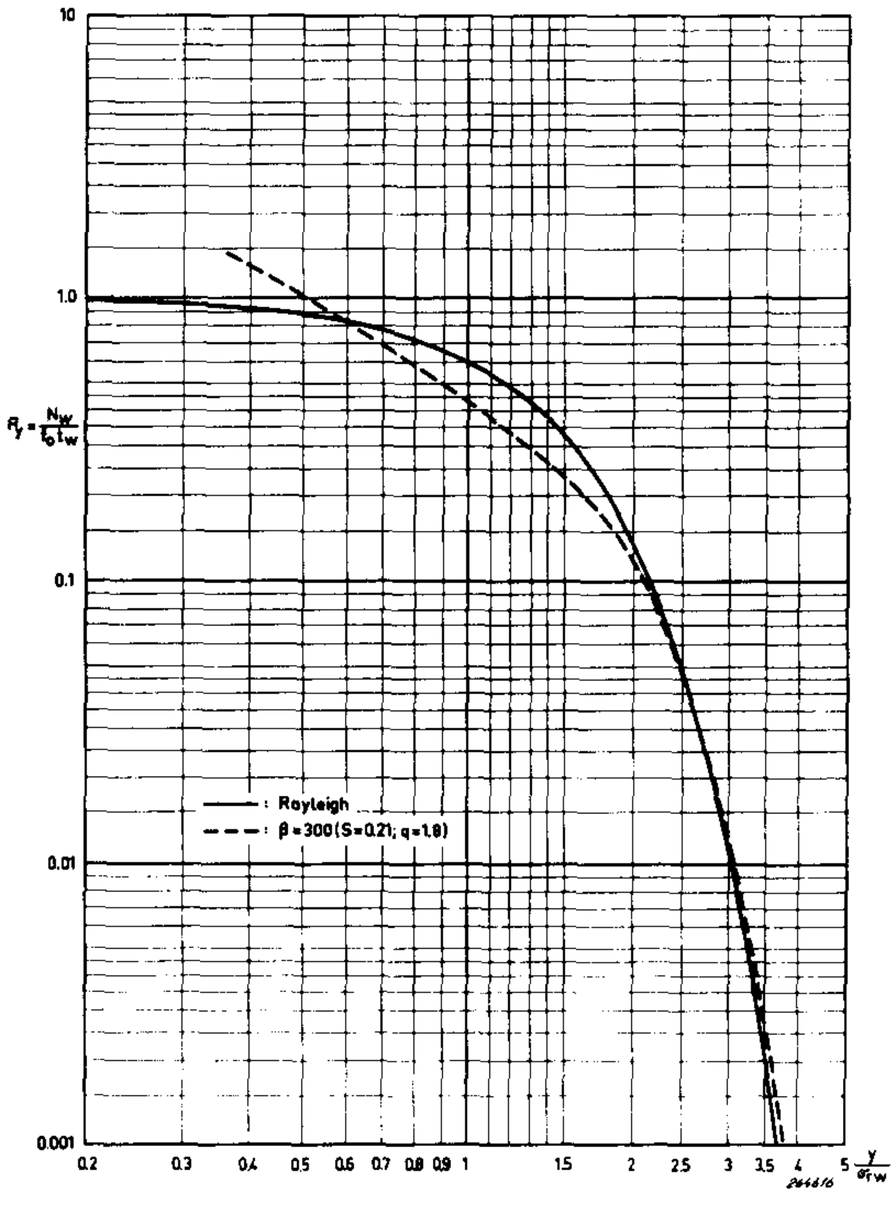

b)

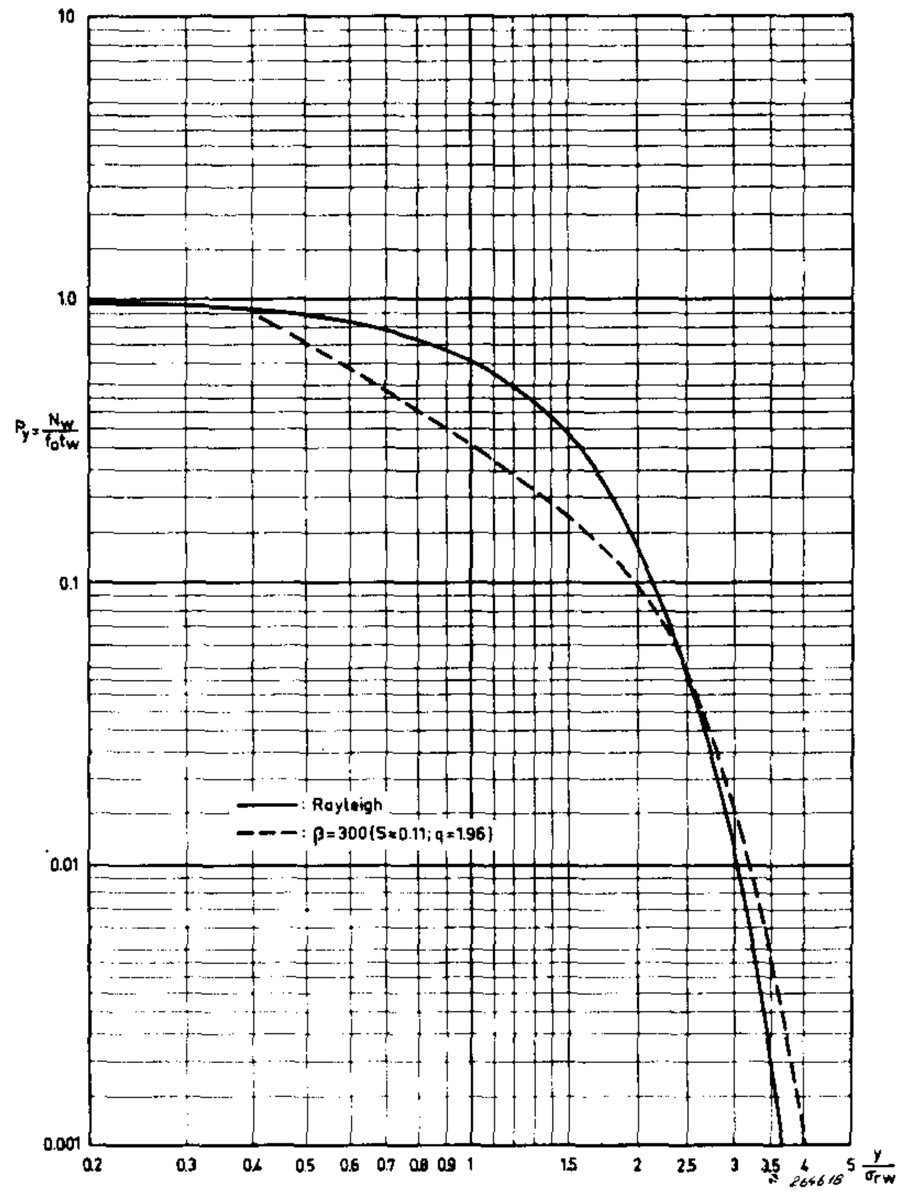

c)

Fig. 8a) Distribution matching for slow sweep random test.

b) Distribution matching for moderately accelerated sweep random test.

c) Distribution matching for sweep random test with six fold reduction in test time.

approximately the same number of acceleration response peaks during the sweep random test as occurs during the wide band random test throughout the critical region from two to three times the wide band rms response acceleration.

The result of such matching is to reduce the test time factor, s, by a relatively large amount, and increase the level factor q, by a small amount, while maintaining the number of response acceleration peaks at the critical levels essentially unchanged by an adjustment of the compressor speed of the control equipment.

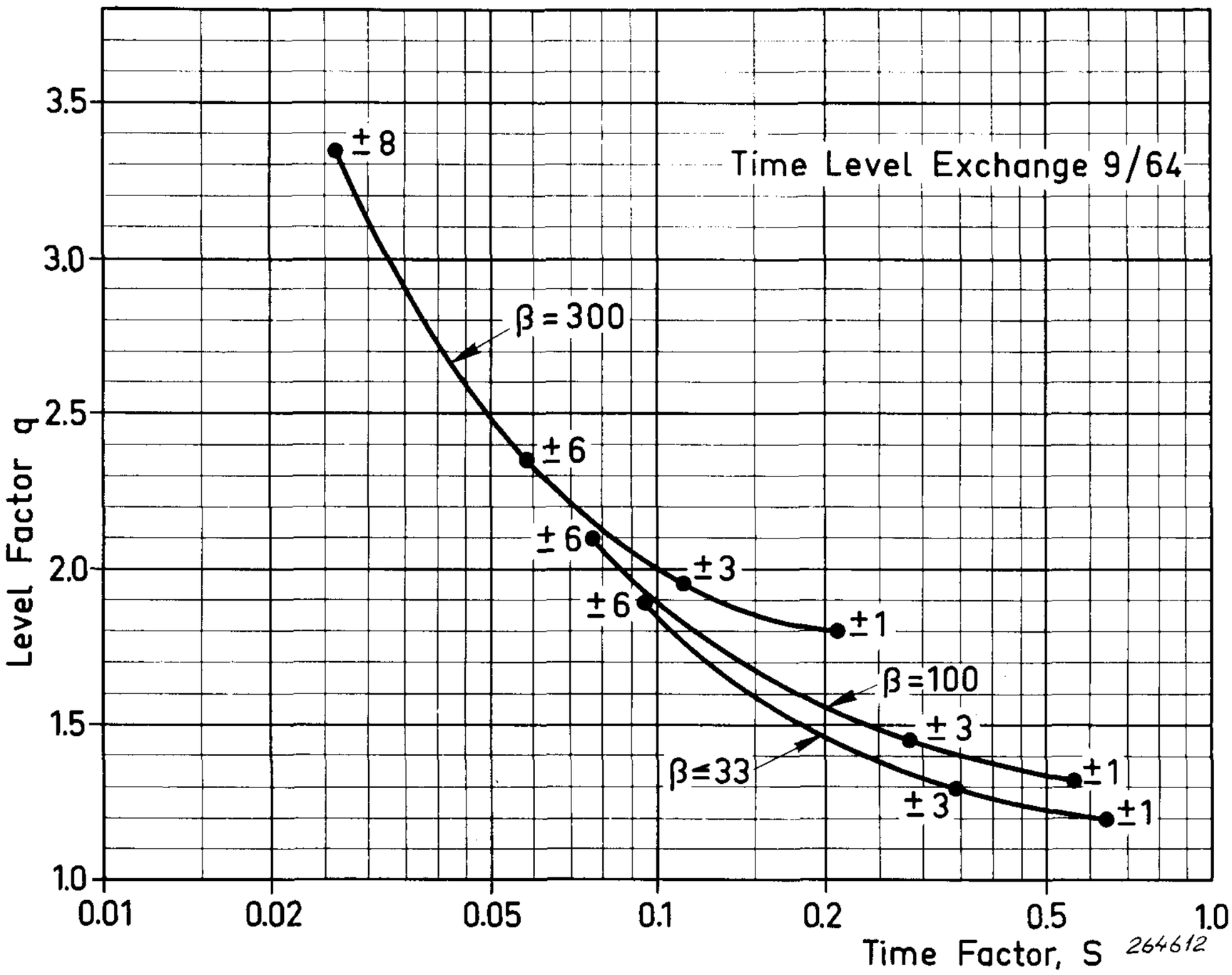

Fig. 9. Time level exchange curves for selection of level factors, q, and time factors, s.

Figure 8a shows the matching for the slow sweep random test. A match with the slow compressor speeds, $\beta \leq 33$, provides the desired distribution of acceleration peaks over a very large amplitude range. Note that the level factor, q, is 1.2.

Figure 8b shows a match which reduces the sweep random test duration to about one third of the time for the slow sweep random test. The number of acceleration peaks is matched within $\pm$ 1 dB from two times to three times the rms response acceleration to the wide band test. Or, in the colloquial language of the test floor, matched within 13 % from 2 to 3 "sigma". Although the test time factor, s, is reduced to o.21, it is not without dis-

advantage, since the level factor, q, must be increased from 1.2 to 1.8, which requires more force from the vibration exciter system.
Figure 8c shows a match which further reduces the test time. The accuracy of the distribution of acceleration peaks is not quite so good, however, becoming $\pm$ 3 dB in the critical 2 to 3 "sigma" region. The test time has been reduced by about another factor of two, to s = o.11, with only a small additional increase in drive level, to q = 1.96. Visual observation of the response acceleration signal on the screen of an oscilloscope shows that the typical fluctuating narrow band character of the response of a resonating circuit to a random excitation is maintained.
The curves of Figure 9, providing sets of values for q and s, summarize the results of many such matches. Three curves are shown, one for slow compressor speeds, $\beta \leqq 33$; one for an intermediate compressor speed-bandwidth relationship, $\beta = 100$, and one for the highest recommended compressor speed-bandwidth relationship, $\beta = 300$. The accuracy of the match, in dB, in the 2 to 3 "sigma" region, is shown by notations beside the dots on the curves.
Although it was possible to obtain a compressor speed-bandwidth relationship, β, equal to 1ooo, this is not recommended since the amplitude distribution is unsatisfactory. High compressor speeds also cause distortion at the lower frequencies. See Appendix B for detailed information.

New Test Approach.
A new test approach is proposed.
Due to the possibilities shown for accelerated testing it is reasonable to first determine what time is available for testing. With this information, the most suitable β-value and test accuracy are determined and the corresponding q and s values found from the curves given in Figure 9.
The control equipment is then adjusted to produce an acceleration gradient of

$$\gamma = q \sqrt{\frac{G}{80}}$$

and the test continues for a time

$$t_n = s \times 20\, t_w \ln \frac{f_H}{f_L}$$

APPENDIX A: DERIVATION OF EQUIVALENT SWEEP RANDOM TEST*)

Objective.
The sweep random test shall cause the same number of stress reversals at each stress level as does the wide band random test. Since for each linear resonance the stresses are proportional to the response acceleration, the

---

*) The derivation in Appendix A is applicable to the normal Rayleigh distribution of acceleration peaks of narrow band random signals. This Rayleigh distribution is produced when the control equipment is adjusted so that the quotient of the compressor speed in dB/sec. and the bandwidth in cps is equal to or less than 33.

number and amplitude distribution of the larger response accelerations for the sweep random test are adjusted until they agree with the number and amplitude distribution of the larger response accelerations for the wide band random test.

Wide Band Random Excitation.

The response of a single degree of freedom system or of a lightly damped mode of a complex structure to a wide band random vibration excitation is

$$\sigma_{rw} = \sqrt{\frac{\pi \ G \ f_o \ Q}{2}} \tag{1}$$

where σ_{rw} is the rms acceleration response, wideband, in g, G is the acceleration density in $g^2/_{cps}$, f_o is the frequency in cps of the responding resonance, and Q is the magnification factor of the resonance.

If a wide band random vibration is filtered to narrow bandwidth, either electrically or mechanically by a resonance, the response is a random vibration of nearly constant frequency but varying amplitude.

The peaks of any narrow band random acceleration response are distributed according to the Rayleigh distribution

$$p_y = \frac{y}{\sigma_r^2} \cdot e^{-\frac{y^2}{2\sigma_r^2}}, \tag{2}$$

where p_y is the probability density of an acceleration peak of magnitude y and σ_r is the rms acceleration response. The probability that an acceleration peak will have a magnitude greater than y is given by the integral of p_y from y to ∞.

$$P_y = \frac{1}{\sigma_r^2} \int_y^\infty y \, e^{-\frac{y^2}{2\sigma_r^2}} \, dy \tag{3}$$

which is

$$P_y = e^{-\frac{y^2}{2\sigma_r^2}} \tag{4}$$

shown in Figure 8.

If the wide band excitation continues for a time t_w, the maximum number of acceleration response peaks is $f_o t_w$. The expected number of peaks which exceed the magnitude y is then

$$N_y = f_o t_w P_y \tag{5}$$

Sweep Random Excitation.

If the same structure is excited by a random vibration with bandwidth much narrower than the bandwidth f_o/Q of the resonance, the response is

$$\sigma_{rn} = H\sigma_e \tag{6}$$

where σ_{rn} is the rms acceleration response, narrow; σ_e is the rms acceleration excitation, and the transmissibility of the structure, H, is given by

$$H = \left| \frac{1}{1 - (f/f_o)^2 + jf/Qf_o} \right| \tag{7}$$

As the center frequency of the sweep random excitation approaches f_o, the response increases until it reaches a maximum rms magnitude $Q\sigma_e$.
If the center frequency of the narrow band random excitation changes so slowly that the resonance can build up to full response, and also if the time constant of the compressor in the control loop is so slow that the amplitude distribution is unaffected by compressor action, the probability that an individual acceleration peak will exceed the level b is given by

$$P_b = e^{-\frac{b^2}{2\,H^2\,\sigma_e^2}} \tag{8}$$

A logarithmic frequency sweep rate is defined by

$$\frac{df}{dt} = rf \tag{9}$$

In the time period dt, the number of acceleration peaks exceeding the level b is

$$dN = P_b f dt = P_b \frac{df}{r} \tag{10}$$

The total number of peaks exceeding the level b becomes

$$N_b = \frac{1}{r} \int_0^\infty e^{-\frac{b^2}{2\,H^2\,\sigma_e^2}} df \tag{11}$$

Make the substitution $e^x = \frac{f}{f_o}$, expand the exponent, and discard small terms. (11) then becomes

$$\begin{aligned} N_b = \frac{1}{r} \int_0^\infty e^{-\frac{b^2}{2\,\sigma_e^2}\left[4x^2 + \frac{1}{Q^2}\right]} df = \\ \frac{f_o}{r} \int_{-\infty}^\infty e^{x - \frac{b^2}{2\,\sigma_e^2}\left[4x^2 + \frac{1}{Q^2}\right]} df \end{aligned} \tag{12}$$

with the further substitution $y = x - \left(\frac{\sigma_e}{2\,b}\right)^2$, (12) becomes

$$N_b = \frac{f_o}{r} \int_{-\infty}^\infty e^{-\frac{2\,b^2\,y^2}{\sigma_e^2}} e^{-\frac{2\,b^2}{\sigma_e^2}\left[\frac{1}{4\,Q^2} - \frac{\sigma_e^4}{16\,b^4}\right]} dy \tag{13}$$

which integrates to

$$N_b = \sqrt{\frac{\pi}{2}} \frac{\sigma_e}{b} \frac{f_o}{r} e^{-\frac{2\,b^2}{\sigma_e^2}\left[\frac{1}{4\,Q^2} - \frac{\sigma_e^4}{16\,b^4}\right]}. \tag{14}$$

(14) expresses the number of response peaks exceeding the level b when a resonance is excited with a narrow band random excitation, with bandwidth much narrower than f_o/Q and rms value σ_e, which is swept past the resonance

frequency f_o at a sweep rate $df/dt = rf$, when the control compressor time constant is long.

It is convenient to normalize (14) by dividing by the total number, N_r, of acceleration cycles occurring during the sweeep through the bandwidth of the resonance, $f_o\left(1 - \frac{1}{2Q}\right)$ to $f_o\left(+ \frac{1}{2Q}\right)$.

$$N_r = \int f\,dt = \int_{f_o\left(1-\frac{1}{2Q}\right)}^{f_o\left(1+\frac{1}{2Q}\right)} df/r = \frac{f_o}{rQ} \qquad (16)$$

After normalization, (14) becomes

$$\frac{N_b}{N_r} = \sqrt{\frac{\pi}{2}}\,\frac{Q\sigma_e}{b}\; e^{-\frac{1}{2}\left(\frac{b}{Q\sigma_e}\right)^2\left[1-\frac{1}{4Q^2}\left(\frac{Q\sigma_e}{b}\right)^4\right]}$$

which is plotted in Figure 6.

The curve of Figure 6a) may be superimposed on the integrated Rayleigh curve of Figure 6b), to give Figure 7. The two curves are close in the critical region between $\frac{b}{\sigma_{rw}} = 2$ and $\frac{b}{\sigma_{rw}} = 3$, and deviate little from $\frac{b}{\sigma_{rw}} = 1$ to $\frac{b}{\sigma_{rw}} = 4$.

The fact that these curves can be made to nearly coincide is important because it permits the sweep random test to closely reproduce all of the damage-producing response acceleration peaks over the entire amplitude range.

The sweep random sweep rate and excitation level are determined from the relative position of the graphs when the curves coincide.

The excitation for the sweep random test is found by equating the horizontal axes of Figure 7,

$$\frac{y}{\sigma_{rw}} = q\,\frac{b}{Q\sigma_e} \qquad (17)$$

The ratio, q, of the positions of the horizontal axes is 1.2 for the case of slow compressor speed. Since for a wide band excitation the rms response, σ_{rw}, is given by (1), the sweep random acceleration excitation becomes

$$\sigma_e = q\sqrt{\frac{\pi\,G\,f}{2\,Q}} \qquad (18)$$

Since this acceleration excitation varies as $f^{1/2}$, it is convenient to introduce a new parameter, the acceleration gradient, γ, which is independent of frequency and is maintained constant by action of the compressor during the sweep random test.

$$\gamma = \frac{\sigma_e}{\sqrt{2\,\pi\,f}} \qquad (19)$$

The excitation level for the sweep random test may then be expressed as an acceleration gradient

$$\gamma = q \sqrt{\frac{G}{4\,Q}} \tag{20}$$

Since the magnification factors, Q, of the many resonances in a specimen are unknown, a median value must be arbitrarily chosen which is approximately right for all resonances. A value of 20 is recommended for Q, which keeps the response within $\pm$ 3 dB for the normal Q range of 10 to 40 and within $\pm$ 7 dB for the extreme range 4 to 100. Note that the test is conservative, the high Q resonances are the ones tested excessively, the low Q, more resistant resonances are the ones inadequately tested. Using this recommended value, the acceleration gradient for the sweep random test is

$$\gamma = q \sqrt{\frac{G}{80}} \tag{21}$$

where G is the wide band acceleration density in g^2/cps.
The sweep rate is found by matching the vertical axes of Figure 7

$$\frac{N_w}{f_o\, t_w} = s\,\frac{N_b}{N_r} = \frac{s\ r\ N_n\ Q}{f_o} \tag{22}$$

The ratio, s, of the vertical axis positions is o.65 for the case of slow compressor speed.
Since it is desired that the number of peaks at each level be the same, $N_n = N_w$, and the sweep rate becomes

$$r = \frac{1}{s\ Q\ t_w} \tag{23}$$

Using (9), the total sweep random test time, t_n, is

$$\frac{1}{r}\int_{f_L}^{f_H} \frac{df}{f} = \frac{1}{r}\ \ln\ \frac{f_H}{f_L} \tag{24}$$

where f_L and f_H are the lower and upper limit frequencies, respectively. Using r from (23) this becomes

$$t_n = s\ Q\ t_w \ln \frac{f_H}{f_L} \tag{25}$$

Using the recommended value of 20 for Q, the sweep random test time becomes

$$t_n = s \times 20\ t_w \ln \frac{f_H}{f_L} \tag{26}$$

where t_n is the sweep random test time in minutes for a wide band test time t_w in minutes, and f_H and f_L are the upper and lower frequency limits.

Bandwidth.

Whenever possible, a narrow test bandwidth, perhaps 3 cps, is chosen. Such a narrow bandwidth requires a relatively slow compressor speed if the high acceleration peaks are not to be compressed undesirably. However, for some tests it may be necessary to sweep rapidly through frequencies where high Q resonances exist. If this is so, then wider bandwidths permit faster compressor speeds and improved correction.

These wide test bandwidths require modification of the test procedure at those low frequencies where the test bandwidth exceeds the bandwidth of the resonant response. A first approximation, exact if the reaction of the resonance on the vibration exciter is negligible, is derived as follows:

If the narrow band excitation is much wider than the resonance, the rms low frequency response acceleration is like the response to a wide band excitation of (1) and becomes

$$\sigma_{rLf} = \sqrt{\frac{\pi \, G_n \, f_o \, Q}{2}} \tag{27}$$

where

$$G_n = \frac{\sigma_{eLf}^2}{B} \tag{28}$$

and σ_{eLf} is the low frequency rms acceleration excitation.

If the rms response acceleration of the prototype wide band test, σ_{rw}, is equated to the low frequency response acceleration of (27), the low frequency acceleration excitation of (28) then becomes

$$\sigma_{eLf} = \sqrt{BG} \tag{29}$$

where G is the acceleration density of the wide band test and B is the bandwidth of the sweep random test.

The low frequency excitation (29) equals the high frequency excitation of (18) at the frequency

$$f = \frac{2\,BQ}{q^2\,\pi} \tag{30}$$

Below this frequency the excitation acceleration is kept constant at the value of (29) and above this frequency the acceleration gradient is kept constant at the value of (20).

APPENDIX B

At the lower frequencies, high compressor speeds tend to distort the wave form of the oscillator output. Figure B1 shows the distortion caused by compressor speeds of 1ooo dB/sec, 300 dB/sec, and 100 dB/sec on both sine and 3 cps bandwidth random signals at both moderate and high compression levels.

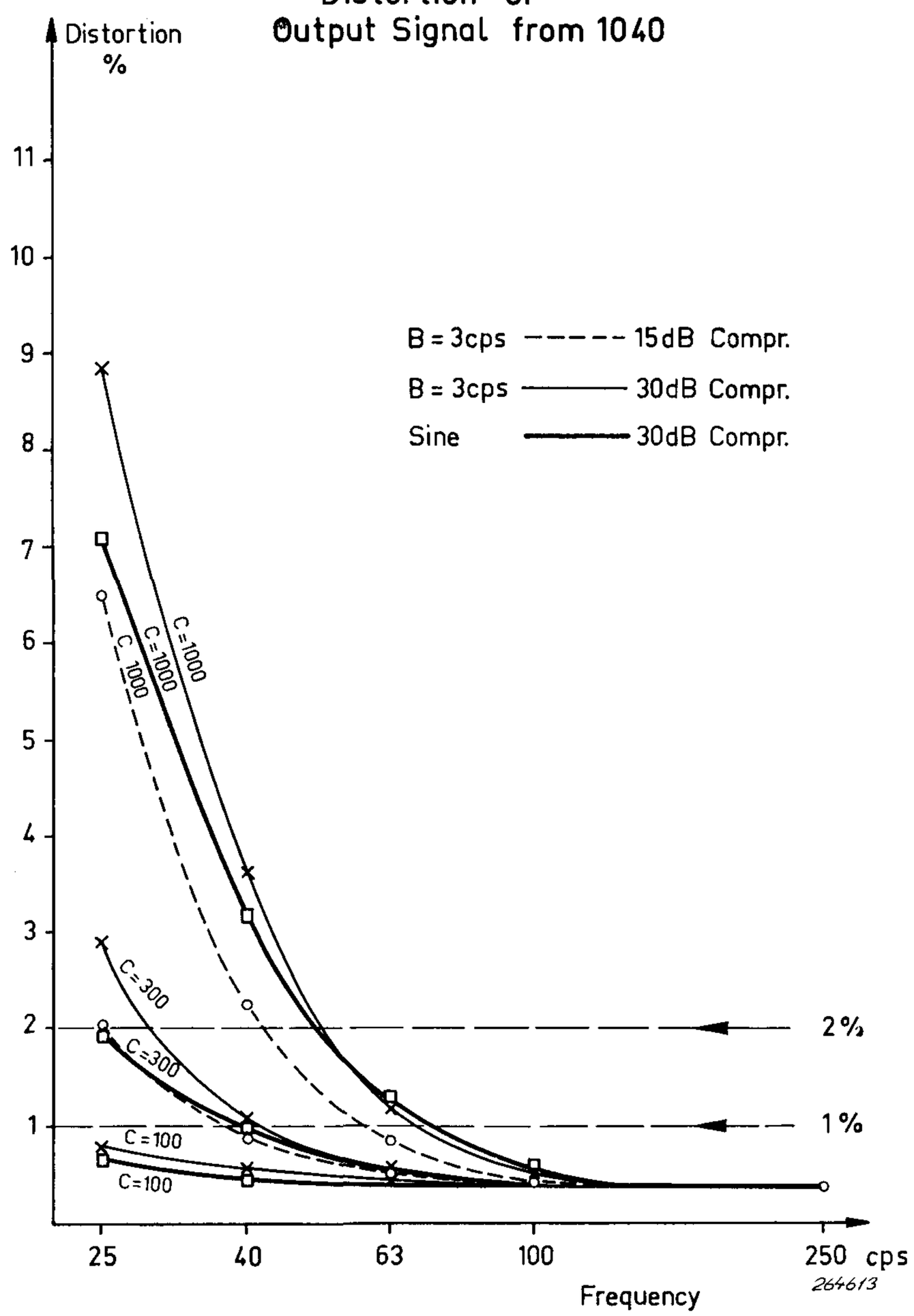

Fig. B.1. Distortion of control equipment signal with high compressor speeds.

REFERENCES:

BOOTH, G. B.: Sweep Random Vibration. Proc. Inst. of Environmental Sciences, April 1960, and Environmental Engineering Quarterly, London, September 1963.

BROCH, J. T.: An Introduction to Sweep Random Vibration. Brüel & Kjær Technical Review, no. 2-1964.

OLESON, M. W.: A Narrow Band Random Vibration Test. Shock and Vibration Bulletin, Part I, December 1957.

The Frequency Response Tracer Type 4709

Some notes on the most significant design problems and their solutions.

By *S. E. Fauerskov*, Development Engineer.

ABSTRACT

This article contains a fairly thorough description of some of the main design features of the Frequency Response Tracer Type 4709. Specific emphasis is given to the logarithmic amplifiers and the frequency detecting circuits. Finally, various possibilities for using different signals for frequency and amplitude indication are discussed on the basis of their applications.

SOMMAIRE

Cet article contient une description très complète de quelques unes des caractéristiques de conception du Traceur en Réponse de Fréquence type 4709. On s'étend particulièrement sur les amplificateurs logarithmiques et les circuits de traduction de fréquence. Finalement on discute diverses possibilités d'emploi de différents signaux pour l'indication de la fréquence et de l'amplitude, eu égard à leurs applications.

ZUSAMMENFASSUNG

Es werden die Konstruktionsmerkmale des Pegelbildgerätes Typ 4709 beschrieben. Näher behandelt wird die Arbeitsweise des logarithmischen Verstärkers und der Frequenz-Meßschaltung. Schließlich werden einige spezielle Anwendungsfälle behandelt, bei denen der Frequenz- und Amplituden-Meßschaltung unterschiedliche Signalformen zugeführt werden.

Main Design Considerations.

The apparatus should be able to draw a curve that would show the voltage level of an audio frequency signal fed to the input, as a function of the frequency. The screen should be large enough to allow legibility of curves at a relatively great viewing distance.

Furthermore, for the sake of versatility only one input channel should be necessary for the indication of both signal level and frequency, the frequency indication being independent of the amplitude within the measuring ranges of the instrument.

The Y-scale of the graph should cover a 25 dB and a 50 dB range logarithmically (linear dB scale) as well as a normal linear voltage range.

The X-scale should cover the frequency range 20 Hz to 20000 Hz logarithmically and for hearing aid and telephone measurements etc. a range of 200 Hz to 5000 Hz.

The performance should be such that direct measurements could be performed with sufficient accuracy not only in production control application but also in the laboratory.

X-Y Plotting.

A 14″ 90° monitor tube with a 110° deflection yoke has been chosen as the indicator. Thereby a rectilinearity of better than ± 1 mm has been accomplished. The screen has a long-persistence electro-luminiscent layer. A snap-

lock mounted frame facilitates the interchangeability of scales for different frequency ranges.

DC Amplifiers for X and Y-Deflection.
A highly stable symmetrical DC amplifier provides a constant current source for the Y-deflection yoke, thus avoiding any effect of the temperature sensitive coil resistance upon the current in it. To obtain zero signal level at the bottom of the Y-scale, the signal of the Y-DC amplifier is biased from a stable floating DC-source.
To minimize losses (and hence power consumption and temperature rise) a special DC power amplifier circuit has been employed. The principle is shown in Fig. 1.

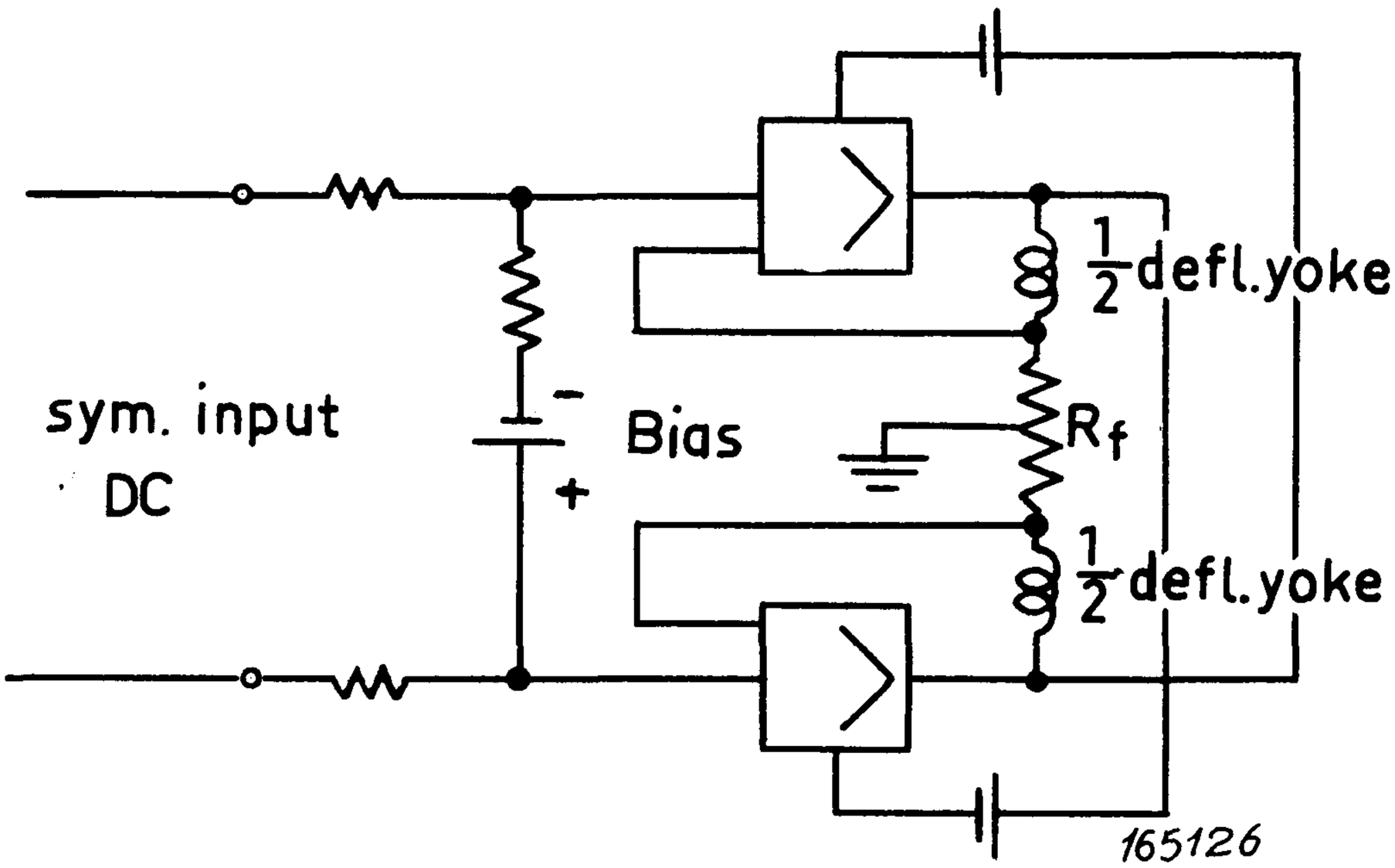

Fig. 1.

A symmetrical DC signal is fed to two current amplifiers, the outputs of which are connected through the two halves of the deflection yoke and the feedback resistor R_f. Two independent and floating voltage sources supply the power necessary to drive the amplifiers. It is seen, that the current in the amplifiers flows through the output load from either side, and that if the currents in the amplifiers are equal, no current will flow in the deflection coil. Now, if the input voltage is zero, voltage across R_f is zero (series feedback) and consequently the output current is zero. The voltage across R_f will closely follow the input voltage up to saturation of the output stage, which occurs when the current in one amplifier output is zero, while it is doubled in the other. A temperature stable wire-wound resistor has been chosen for R_f, as in practice the output current v.s. input voltage stability depends solely on R_f.
The inputs of the Y and X DC amplifiers are fed from DC voltage sources

proportional to the logarithm of the input signal voltage and frequency respectively.

Logarithmic Amplifiers.

A logarithmic amplifier is required to give an output which is proportional to the logarithm of the input voltage i.e.

$$V_{out} = k \log V_{in}$$

where k is a constant. This equation would be represented by a straight line in Fig. 2.

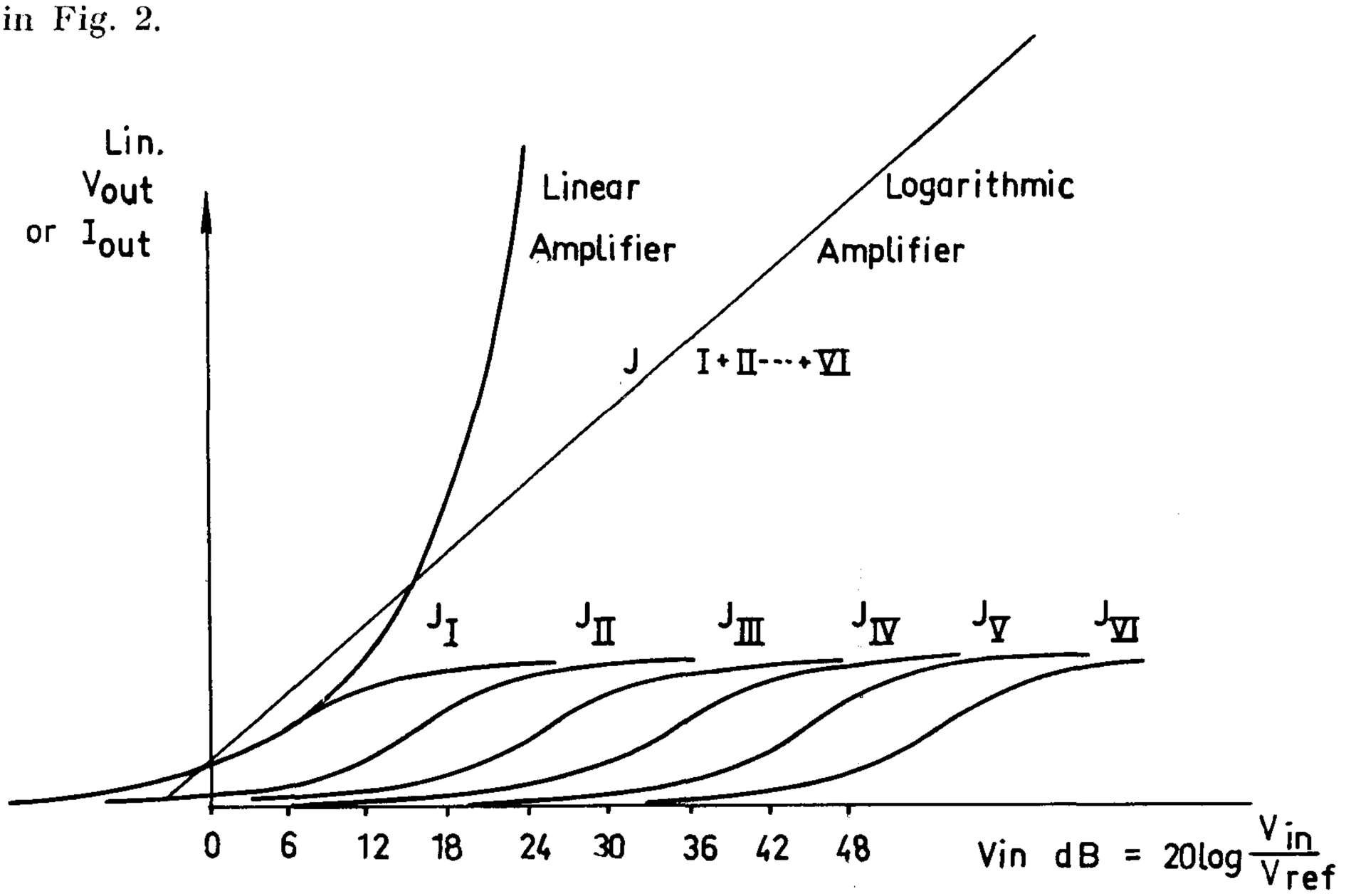

Fig. 2.

In the past, different solutions have been used to realize this function, including back biased diodes in the feedback loop of amplifiers, logarithmic compressors as well as the utilization of the logarithmic function of the leakage current of zener diodes below the zener voltage. In general, however, these solutions suffer from either being logarithmic in a too small dynamic range, having bad stability with temperature, or serious frequency limitations. Therefore, a logarithmic amplifier that could solve these problems, had to be developed. The basic principle has already been used in radar receivers, but special considerations had to be taken into account in order to adapt it for A.F. application.

The principle of operation of such an amplifier is as follows:

The output from a linear amplifier is indicated in Fig. 2 on a linear scale as a function of the input on a logarithmic scale. If the output from such a linear amplifier is amplitude limited its characteristic is changed into that of curve J_1. Fig. 3 shows a cascade coupled amplifier with an output for each

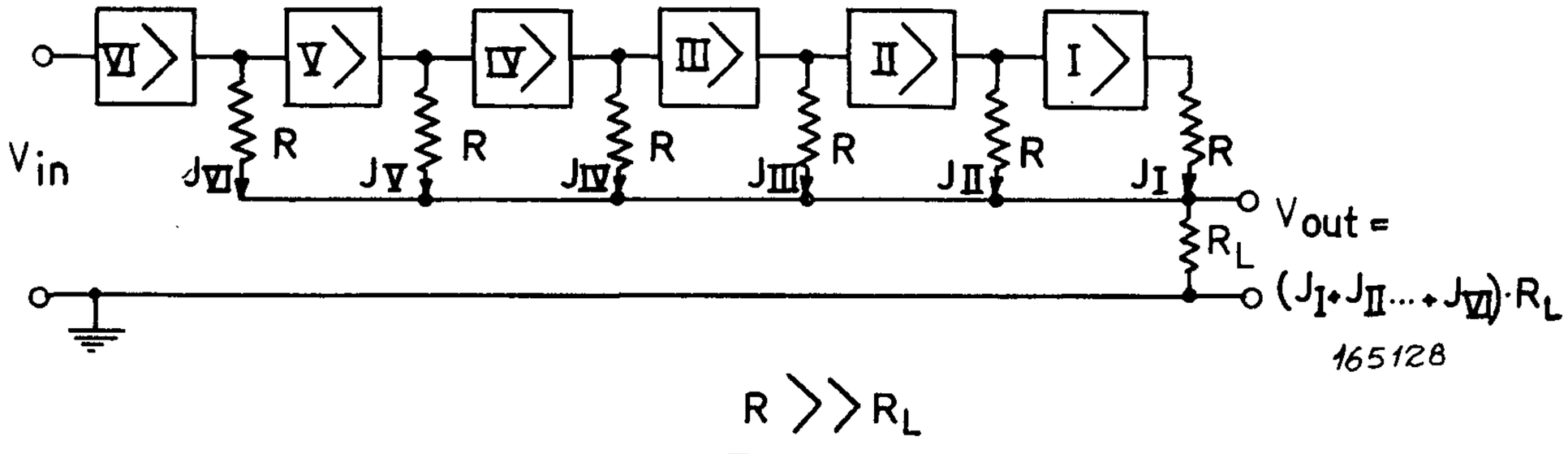

Fig. 3.

stage as used in the Frequency Response Tracer. All outputs are connected to one common load through resistors, R, which are large compared to the load resistor, to accomplish summing of the outputs. The output voltage of each stage is limited and thus the curves J_1, J_{II}, ... J_{VI} may be drawn in on Fig. 2 with horizontal spacing equal to the amplification per stage, 10 dB in the case shown.

Choosing the correct amount of limiting and amplification per stage it is possible to obtain a sum curve $J_1 + J_{II}$ .... $+ J_{VI}$ with very small deviation from a straight line, and thus the output is closely proportional to the logarithm of the input signal.

The curves shown in Fig. 2 are valid for the 50 dB dynamic range of the Tracer. The stage amplification is 10 dB. To obtain a 25 dB range, the stage amplification is changed to 5 dB. The curves J_1, J_{II} .... J_{VI} then have a 5 dB spacing and the sum curve (straight line) will have twice the slope shown. When changing from 10 to 5 dB amplification per stage 25 dB is lost in the total amplification. Therefore if the zero level is required to be the same, an extra amplification of 25 dB must be provided. A linear amplifier is used for this. For the 50 dB range the signal to the input of the logarithmic amplifier is taken from an input cathode follower while the linear amplifier is disconnected. For the 25 dB range the signal comes from the cathode output of the linear amplifier.

Special provisions have been made to make the amplifier suitable for low frequency application. The limitation of the output from each stage is performed by saturating the stage. When a stage is saturated, the DC level at the collector is not allowed to change. This would cause charging of the coupling capacitor to the following stage and consequently a large delay for a sudden decrease of input signal would result, since the time constants of the interstage couplings have to be high. This effect has been reduced to practically zero by proper setting of the working point resulting in symmetrical clipping of the signal. Since the peak output voltage from the stage is directly proportional to the battery voltage, a 24 V reference voltage for stabilization of the latter is obtained by means of four 6 V zener diodes connected in series. A 6 V zener diode has a temperature constant very close to zero, and these have been selected to give a sum voltage of 24 V $\pm$ 0.5 V.

The stability with temperature is measured to be better than o.2 % from 20° C to 50° C.

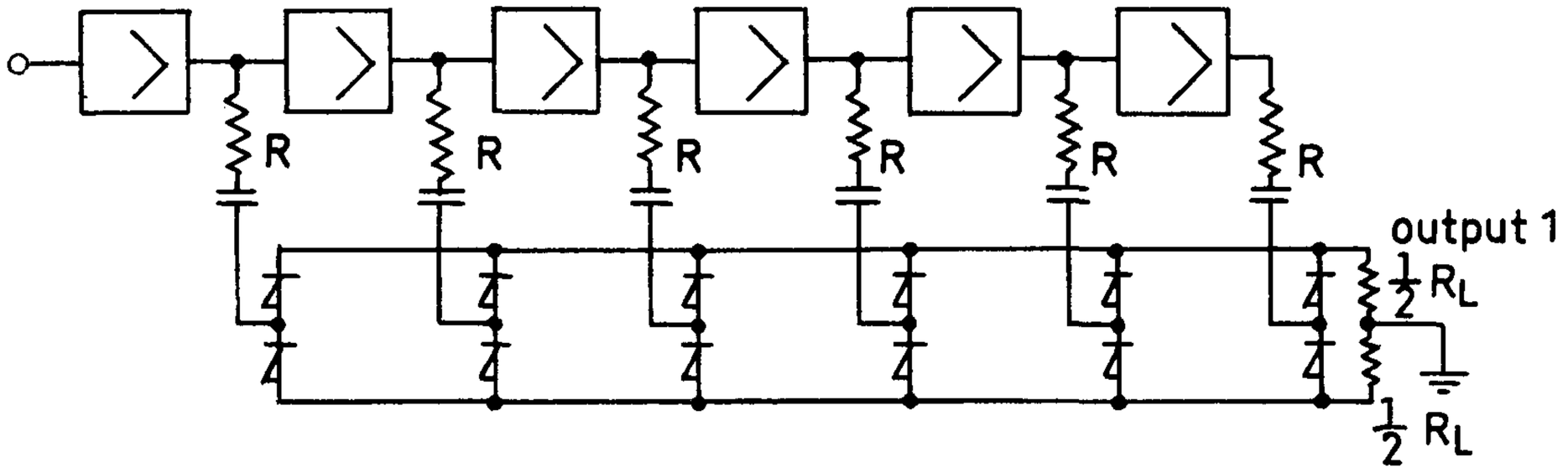

165123

Fig. 4.

Two diodes after each stage output provide symmetrical DC output in conjunction with a symmetrical common load as shown in Fig. 4. As each stage contains only one transistor, the output from one of the stages is in opposite phase of that from the frequency stage. The signal relations are shown in Fig. 5.

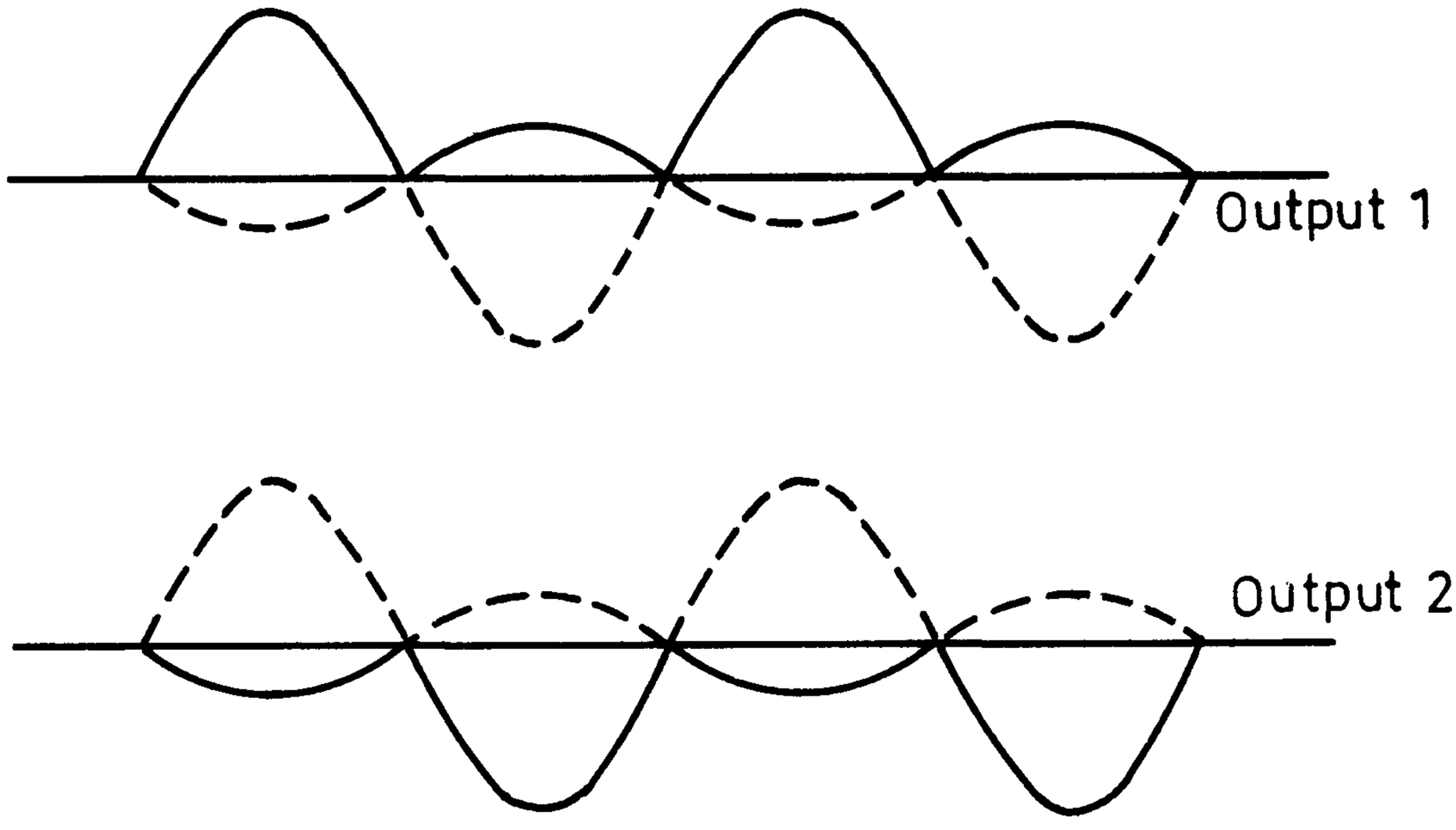

165125

Fig. 5.

It is seen when the stages are saturated as the input signal increases, starting at the end stage, their contribution to ripple is minimized, because their output waveforms will be almost square. Due to the phase inversion in the stages the rectified signal ripple frequency will be mainly of twice the signal frequency.

Frequency Detecting Circuit.

It is required from this circuit, that the output DC signal is proportional to the logarithm of the input frequency.

$$V_{out} = k \log f$$

where k is a constant. This is obtained by means of a special filter network, which will be described later. Also V_{out} must not depend on the input signal amplitude.

The latter requirement is taken care of by a bistable multivibrator which switches over for a very small voltage, i.e. in practice at the zero crossings of the signal. The output from this multivibrator could now in a conventional manner be sent through a suitable high or lowpass filter with following rectification and smoothing. There is, however, an additional requirement to the X-deflection voltage. There must be no ripple. A combination of X and Y ripple results in poor quality indication at the lower frequencies. The consequent requirement to rectification and smoothing collides with a requirement for quick indication. An acceptable ripple at 20 Hz (c/s) would necessitate a smoothing filter giving a delay of about o.5 seconds. A controlled signal rectifier on the principles described below, was developed to answer the requirements for quick indication as well as low ripple.

In a conventional averaging rectifier almost the full half cycle of the signal is impressed upon the DC voltage which is supposed to be constant during this time. In the rectifier employed here the charging condenser is disconnected during the main part of the half cycle. A short pulse samples the instantaneous amplitude at its position in the cycle. Then the charging condenser is disconnected and is now loaded solely by a following DC amplifier. The time constant can easily be made large enough for the voltage to be practically constant over a period for the lowest frequency in question. A sudden change in the input signal frequency will result in a change of charging condenser potential for the pulse immediately following. The above principles are used in the frequency detecting circuit in the following way: (see Fig. 6).

The square wave signal (a) from the multivibrator is differentiated (b), and used as inputs for two monostable multivibrators of opposite polarity. This results in the signal (c) and (d) where $\Delta t < T/2$ for the highest frequency in question. ($T = 1/f$ where f is the input frequency). Now (c) and (d) are differentiated, (e), and fed to a bistable multivibrator. As the multivibrator switches over only when the incoming pulse is of opposite polarity to the previous pulse, we obtain (f) with a delay Δt relative to (a) and the pulses (c) and (d) placed in time at the end of their particular half period, independent of signal frequency. Finally, (f) passes through a suitable high-pass filter whereby (g) is obtained, whose final instantaneous value increases with increasing frequency. The sampling of the final instantaneous value is taken care of by a gate which is controlled by the pulses (c) and (d) so that

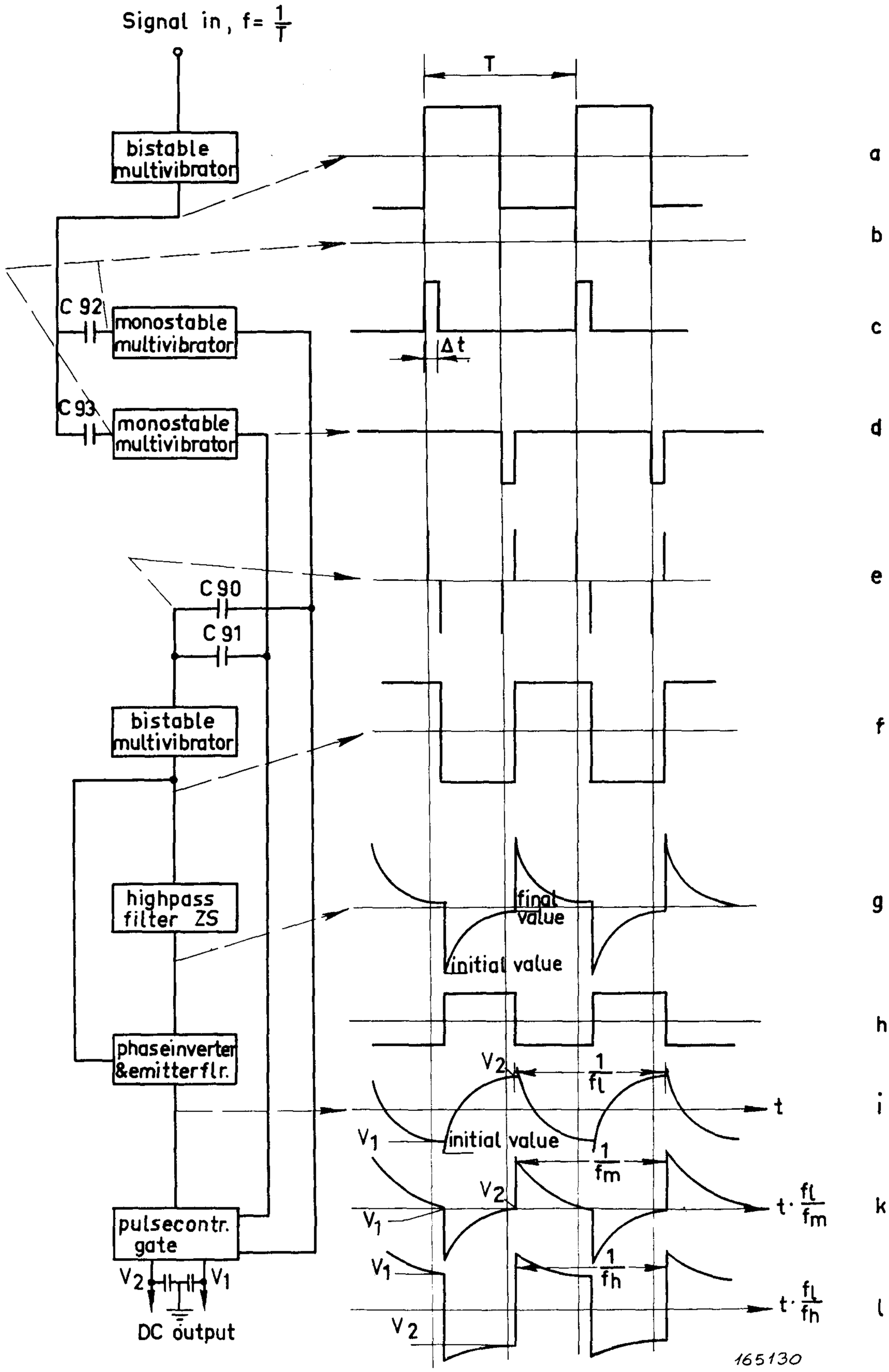
Signal in, f= 1/T
bistable multivibrator
C 92
monostable multivibrator
C 93
monostable multivibrator
C 90
C 91
bistable multivibrator
highpass filter ZS
phaseinverter &emitterflr.
pulsecontr. gate
V2
V1
DC output
T
Δt
final value
initial value
V2
1/fl
t
V1
initial value
1/fm
V2
V1
t · fl/fm
V1
1/fh
V2
t · fL/fh
a
b
c
d
e
f
g
h
i
k
l
165130

Fig. 6.

the symmetrical DC voltages out represent the final instantaneous value of the two half periods.
Between the high-pass filter and the controlled rectifier are inserted a phase inverter and an emitter follower. The phase inverter is used for subtraction of a square wave signal, (h) that is derived from (f) whereby (i) is obtained. It is seen that the final value V_2 has one polarity, and the initial value the opposite, both of about the same size. The signal (i) represents the lowest frequency in the frequency range to be indicated. With increasing frequency the 1/2 period is shortened to the left. Considering V_2 on signal (i) and assuming the period shortened, V_2 will move down the curve, pass through zero and finally at high frequencies end up with the opposite polarity but of about the same size. The same happens to V_1. This means that V_1 and V_2 are opposite but of the same size as they were at the lowest frequency. This is just what is needed for the X-deflection coils since the neutral point of a cathode ray tube is in the middle.
The signal (k) in Fig. 6 represents the signal input to the gate at medium frequency f_m (scale midpoint) with expanded time scale. Signal (l) expresses the highest frequency f_h to be indicated on a time scale expanded by the same factor as the frequency with respect to (i).

High Pass Filter for the Generation of Signal (g).
To clarify how a close approximation to the correct log. frequency function is made in practice, we will first regard a simple circuit.
A square wave signal of $\pm$ Eg is connected through C to R. Regarding a half period the voltage generated across R is governed by the initial value E_1 and the final value E_2.
E_2 is a voltage of special interest since this was the value sampled by the gate to produce the quasi-DC signal for deflection or frequency indication.
We may write the well known

$$E_2 = E_1 \, e^{-\frac{t}{\tau}} \tag{1}$$

where τ = time constant RC and t = 1/2 period time. But E_1 is also a function of time, since it consists of Eg plus the voltage developed across C by charging during the last half period. Therefore

$$E_1 = Eg + (Eg - E_2) = 2\,Eg - E_2 \tag{2}$$

which inserted in (1) gives

$$E_2 = \left(1 + e^{-\frac{t}{\tau}}\right) = 2\,Eg\, e^{-\frac{t}{\tau}}$$

$$E_2 = Eg \, \frac{2}{e^{\frac{t}{\tau}} + 1} \tag{3}$$

The above function $\frac{2}{e^{\frac{t}{\tau}} + 1}$ is calculated with $\tau = 1$ msec. and different values at t.

The results are plotted against $\frac{1}{2\,t}$ = frequency in the graph Fig. 7.

A logarithmic frequency axis and a linear ordinate are chosen for the facility of comparison between the above function and the function wanted, which will represent a straight line with constant slope.

The form of the curve in Fig. 7 resembles that of the partial logarithmic curves obtained for the Y amplifier. It is possible here too, to obtain a curve close to a straight line by superimposing a number of S curves like the one in Fig. 7 with proper horizontal spacing.

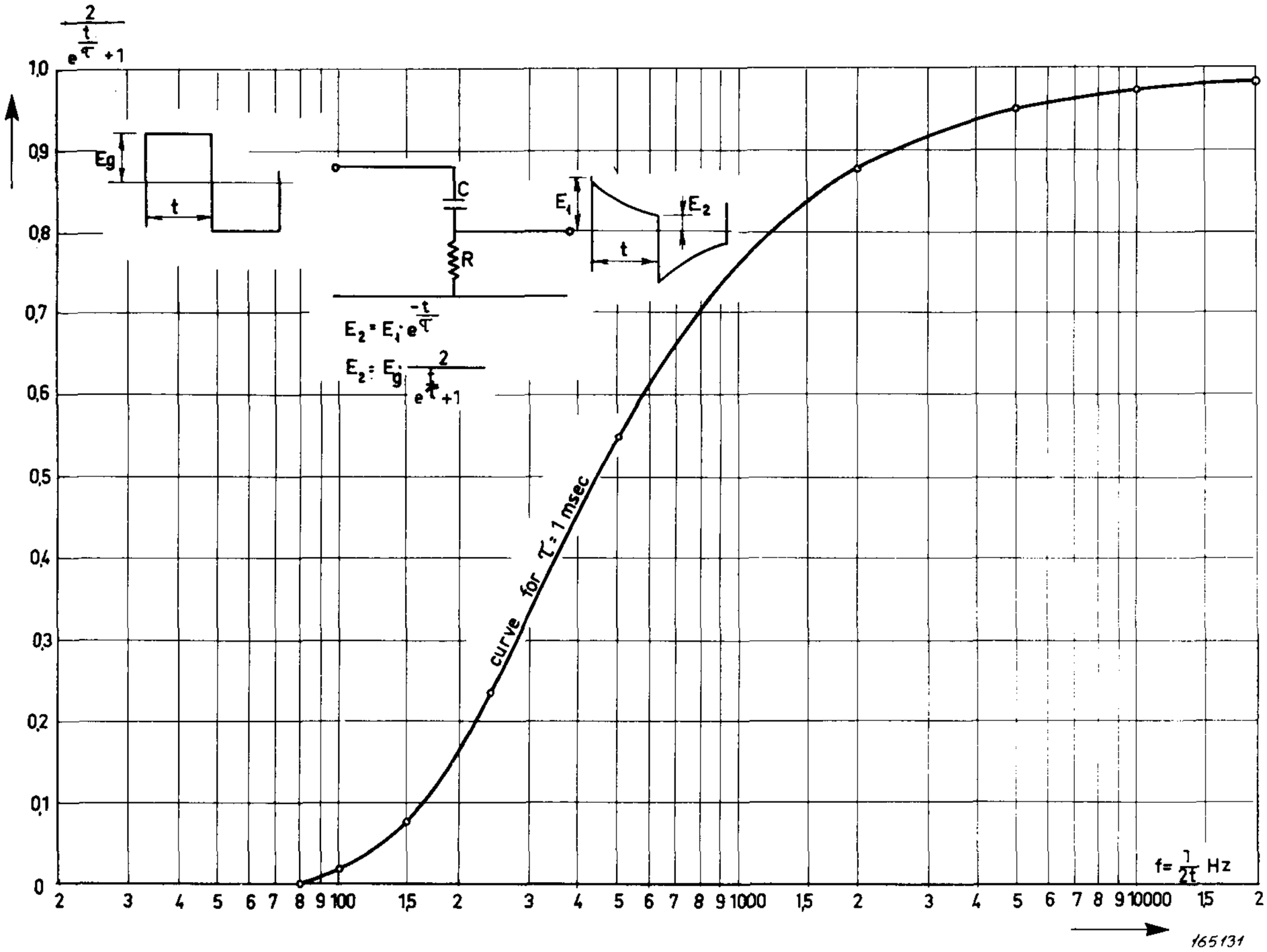

Fig. 7.

A horizontal displacement of the curve is obtained when different values of C are chosen.

Since the voltage across R might as well represent the current through it, superposition of the curves is accomplished by summing the currents, just as in the logarithmic Y-amplifier, see Fig. 8.

From this and eq (3) we obtain

$$E_o = R_L \Sigma I$$

$$\Sigma I = I_1 + I_2 + I_3 + I_4 + I_5$$

$$I_1 = \frac{E_L}{R_1} = \frac{Eg}{R_1} \cdot \frac{2}{e^{\frac{t}{\tau_1}} + 1} \qquad \text{(see Fig. 8 and eq (3))}$$

$$\text{Thus } E_o = 2\,R_2 \times Eg \times \left(\frac{1}{R_1\,(e^{\frac{t}{\tau_1}} + 1)} + \cdots\cdots \frac{1}{R_5\,(e^{\frac{t}{\tau_5}} + 1)} \right)$$

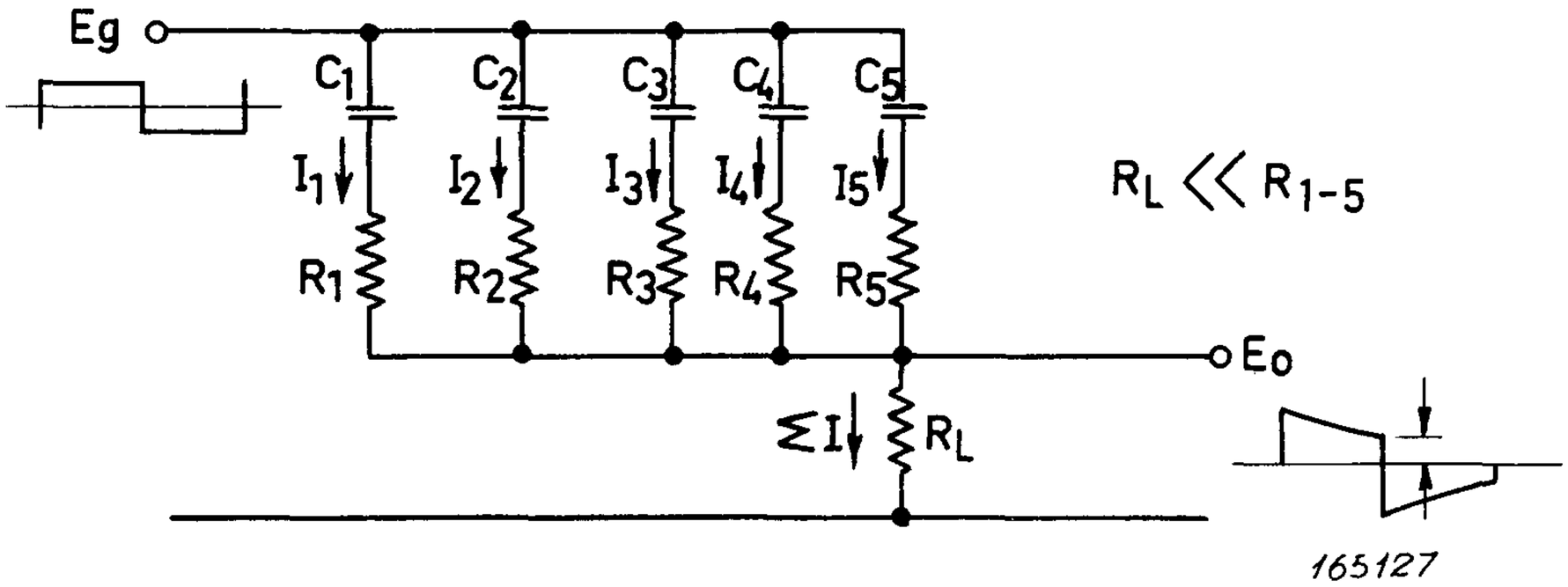

A final "filter" configuration.

Fig. 8.

Practical Design of the Filters.

Since an exact calculation is impractical, dimensioning of the filters is performed by

1) Choosing a suitable voltage level range for E_o considering the components involved in the circuits.
2) Choosing $Eg \gg E_{o\,max}$ depending also on active components available to generate Eg.
3) Choosing the order of $C_{1\text{-}n}$ in a reasonable range for stable polystyrene capacitors.
4) Finding the numbers of partial curves necessary and the spacing between them by graphical means (Fig. 7). Spacing is roughly a factor of 5 between τ's.
5) Determination of $C_{1\text{-}n}$ and $R_{1\text{-}n}$. Roughly a factor of 5 between C's, and all R's equal.
6) Calculation of R_L from the required $E_{o\,max}$, parallel value of R_1 through R_n and Eg. At relatively high frequency $E_2 = E_g$ (eq (3))
whereby

$$\Sigma I \cong \frac{Eg}{R_1 \,//\, R_{2\text{-}n}}$$

$$E_o = \Sigma I \;\; R_L$$

$$R_L = \frac{E_o}{\Sigma 1} = \frac{E_o \;\; R_1 \,//\, R_{2\text{-}n}}{Eg}$$

The conclusion in point (5) holds true only when a large number of curves are used, but the practical filter must contain as few components as possible.

Furthermore the spot deflection on the screen of the picture tube is not a true linear function of current in the deflection coil due to the tangent effect. Due to these facts, the practical filter obtained by adjustments to the closest approach to a logarithmic frequency scale, contains R and C values deviating from the relative values found above. The example of Fig. 8 containing five R-C units has been dimensioned to cover 3 decades of frequency with a maximum deviation from $E_o = K \times \log f$ of less than 1 % of full scale width. The frequency scale graduations of Type 4709 take this into account.

Special Frequency Ranges for the X-Deflection.

The Frequency Response Tracer Type 4709 is delivered with two plug-in units covering the complete audio range 20—20ooo Hz and the range 200—5ooo Hz respectively. The latter range has been chosen to cover telephone equipment and hearing aid measurements.

It may happen, however, that the use of special frequency ranges are desirable and in this respect the plug-in system is very versatile. In the following, a basis for simple calculations of special plug-in units is given.

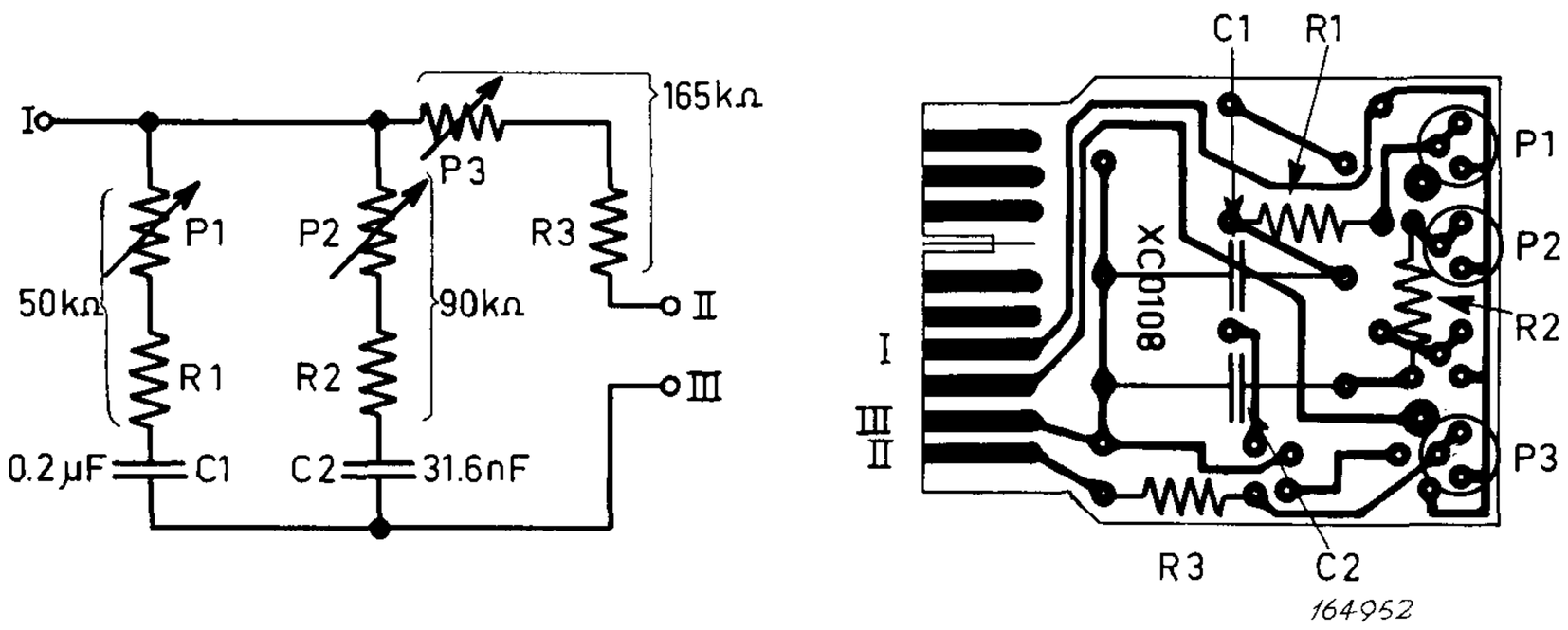

Fig. 9.

An x-deflection filter for the range 20—200 Hz is sketched in Fig. 9. For other one-decade filters the two capacitors may be calculated from the following:

Frequency range f_1—f_2 ($f_2 = 10\, f_1$)

Scale factor $f_1/20 = f_2/200$

The o.2 μF capacitor is changed to

$$\text{o.2/scale factor} = \frac{\text{o.2} \times 20}{f_1} = \frac{4}{f_1} \quad \mu\text{F}$$

The 31.6 nF capacitor is changed to

$$\text{31.6/scale factor} = \frac{31.6 \times 20}{f_1} = \frac{632}{f_1} \quad \text{nF}$$

The resistors will be practically unchanged.

Any frequency range down to one decade may be calculated from the

standard filter components in ZS 0120, ZS 0121 and the one-decade filter described above. These filters may be converted to other ranges simply by changing all the capacitors by the factor of change in question. No change in relative frequency range will take place.

If at the same time a special relative range is wanted, the known filter closest to the one in question and having a larger frequency range is chosen as basis for the design. If the logarithmic mid-frequency is not changed and a new, smaller relative range is desired all impedances, including the $1/\omega C$'s, must be multiplied by the factor of range reduction.

Example:

A range of 100—10ooo Hz is wanted. A ZS 0120 (20—20ooo Hz) is used as a base.

Logarithmic midpoint of ZS 0120 is $\sqrt{20 \times 20ooo} = 630$ Hz.

Logarithmic midpoint of new range is $\sqrt{100 \times 10ooo} = 1ooo$ Hz.

Thus the scale factor for the capacitors will be $\frac{630}{1ooo} = o.63$.

The logarithmic range of ZS 0120 is $\log \frac{20ooo}{20} = 3$.

The logarithmic range of the new filter is $\log \frac{10ooo}{100} = 2$.

Scale factor for all impedances is 2/3.

Factor for resistors is 2/3.

Factor for capacitors is $o.63 \times 3/2 = o.945$, where the factor o.63 is responsible for moving the whole frequency range and the factor 2/3 decreases the range.

The factor for the capacitors is close to 1, and we shall see what the results will be if the capacitors are left unchanged:

Frequency range $100 \times o.945$ to $10ooo \times o.945 = 94.5$ to 9450 Hz. As we know that this type of filter is capable of covering one half decade more at both ends of the range than is used in this case, we leave the capacitors unchanged and displace the range by a factor 1/o.945 just by decreasing the resistance between contacts I and II. See Fig. 10.

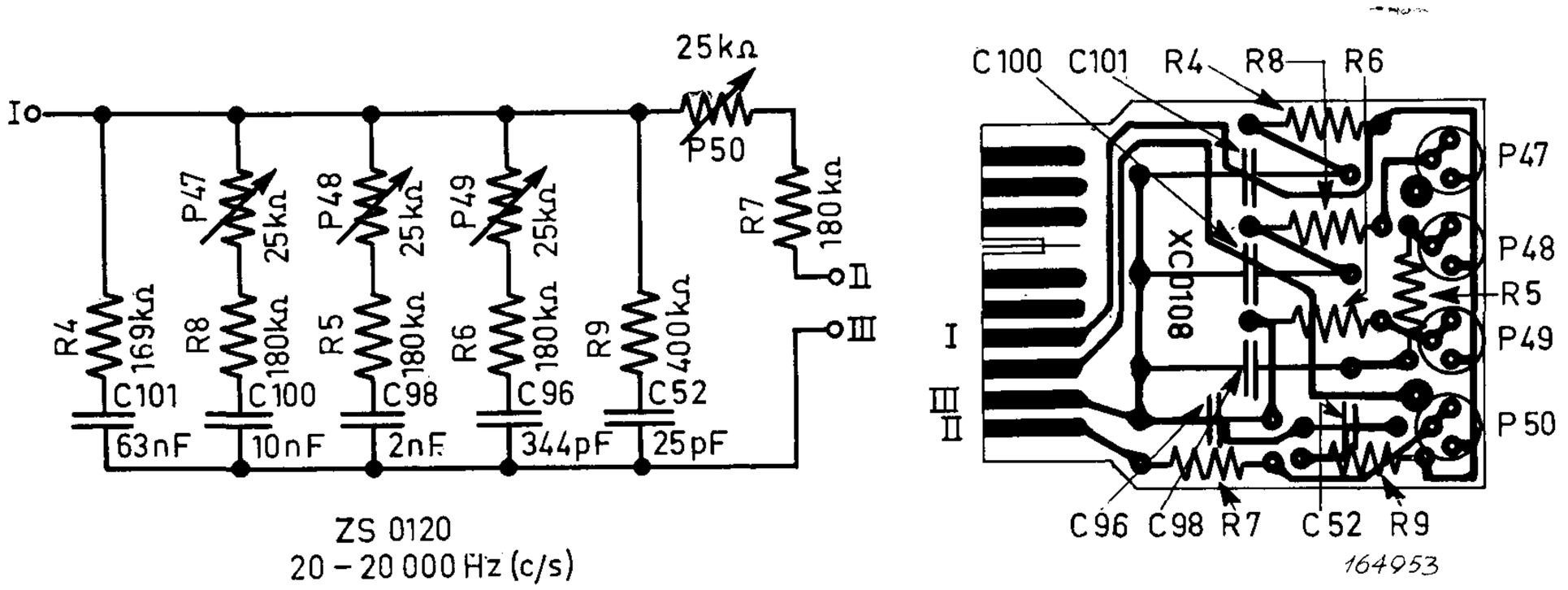

Fig. 10.

Finally the component values of the new filter will be:

R_4	169 kΩ	changed to	169	× 2/3	= 112 kΩ
R_8	180 + 12.5 kΩ	changed to	192.5	× 2/3	= 128 kΩ
R_5	180 + 12.5 kΩ	changed to	192.5	× 2/3	= 128 kΩ
R_6	180 + 12.5 kΩ	changed to	192.5	× 2/3	= 128 kΩ
R_9	400 kΩ	changed to	400	× 2/3	= 267 kΩ
R_7	180 + 12.5 kΩ	changed to	192.5	× 2/3	= 128 kΩ

Half the series potentiometer values must be subtracted from the values for R_5, R_6, R_7 and R_8 so that these values will be:

$$R_5 = R_6 = R_7 = R_8 = 128 - 12.5 = 115.5\ k\Omega$$

To obtain the same stability as that of the standard filters supplied, metal film resistors and polystyrene capacitors should be employed.
Ranges extending higher than 20ooo Hz and lower than 5 Hz are not recommended.

Frequency Scale Multiplication.

If a frequency divider or multiplier is connected between the signal and the "Ext. Freq. Input", the frequency scale is still applicable, just being multiplied by a factor equal to the divider. In this way it is possible to use a signal of one frequency (the measurement frequency) for the Y-amplifier while the actual input frequency to the X-amplifier is converted into a frequency suitable for the purpose and bearing a fixed relationship to the measurement frequency. For instance a simple "by two" divider consisting only of a single bistable stage, will convert the frequency scales of 4709 to 400—10ooo and 40—40ooo Hz respectively. As the "Signal Input" should receive the signal directly, the Y-amplifier actually determines the highest signal frequency that can be measured. This amplifier falls off approximately 1 dB at 100 kHz.
Frequency dividers are available as "building blocks" from many manufacturers. The only requirement is that the output signal should be symmetrical, i.e. with positive and negative half periods of the same duration.

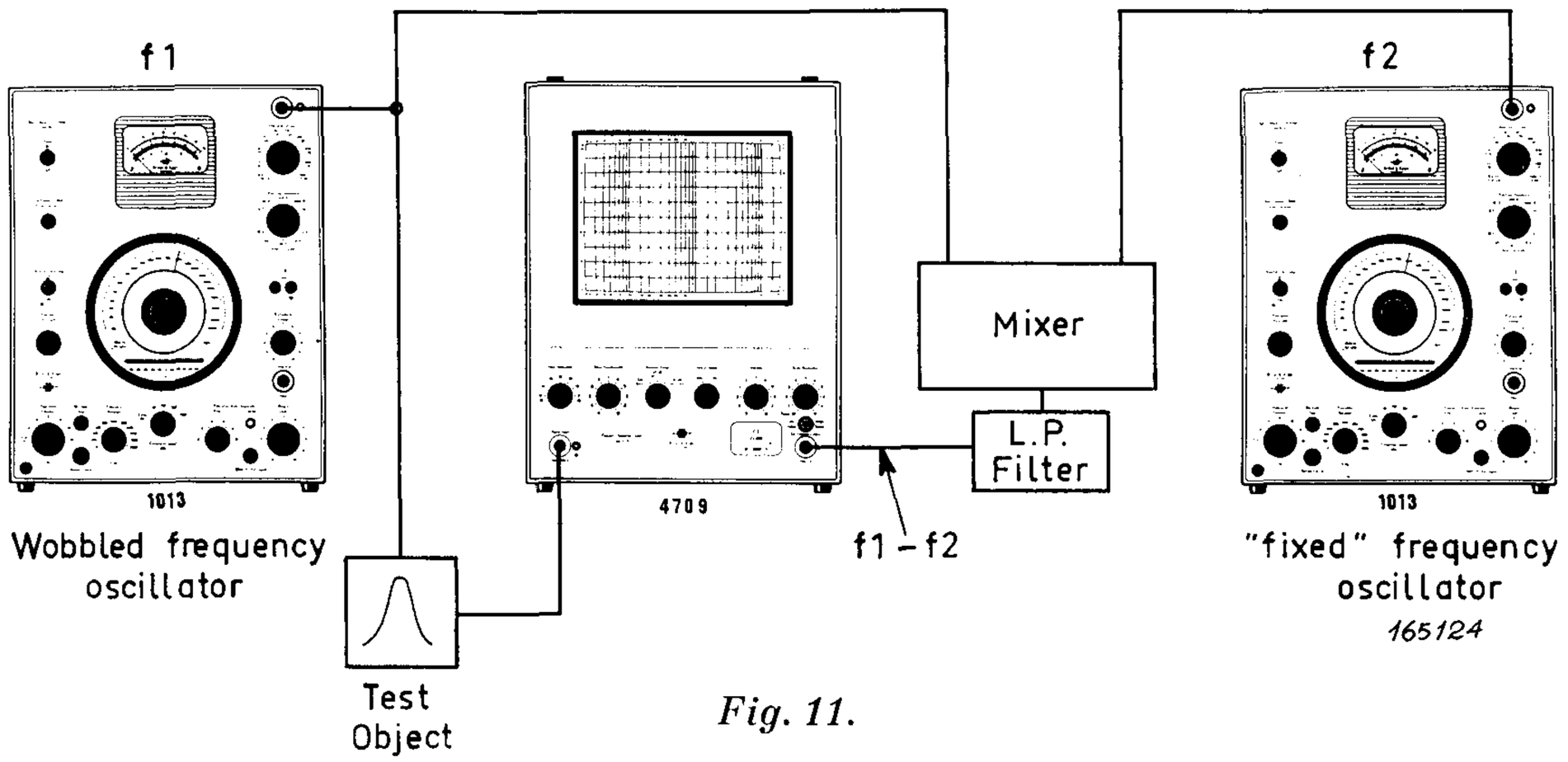

Fig. 11.

"Constant Bandwidth" by Heterodyne Principle.

For measurements on filters for different purposes and with various center frequencies, for instance filters for carrier telephony, the following set up is suggested. (Fig. 11).

Examples:

Filters, having a 4ooo Hz bandwidth with center frequencies ranging from 60 kHz to 120 kHz, are to be checked.

A plug-in unit for 200—5ooo Hz is used for Type 4709. Using the heterodyne arrangement shown in Fig. 11 the wobble oscillator is set to wobble between 60—64 kHz while the fixed oscillator is set to 59 kHz. After mixing the two, and filtering,*) the difference frequency 1ooo to 5ooo Hz controls the Response Tracer. It is seen that any "carrier" frequency can be applied if only the "fixed" frequency follows.

---

*) Mixer stage and filter stage are not supplied by Brüel & Kjær.

News from the Factory

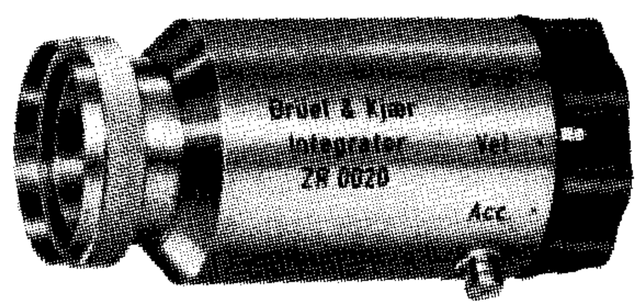

Type ZR 0020

Integrator ZR 0020.

The Integrator, containing two stages of integration, is designed for screwing directly onto a B & K Precision Sound Level Meter Type 2203, effectively converting this into a handy, portable vibration meter, capable of indicating levels of acceleration, velocity and displacement when an accelerometer is employed as a vibration transducer. A slide rule is delivered with the Integrator which may be set to the accelerometer sensitivity and used for direct conversion of dB-readings to units of vibration (metric and British). Accelerometer sensitivities from 10 to 1ooo mV/g are covered.

The components of the RC integrating networks have been chosen to give a low-frequency cut-off (— 3 dB point) at about 5 Hz. This is sufficiently low, since the Precision Sound Level Meter itself has a low-frequency cut-off in the same region. The high-frequency limits are determined by the capacitive coupling between input and output and are about 10 kHz for velocity and 4 kHz for displacement measurements. These ranges are sufficiently large for the majority of applications.

It is also quite possible to use the Integrator with the B & K 1″ Cathode Followers, whereby measurement and analysis of acceleration, velocity and displacement may be carried out with any of the B & K analyzing/indicating instruments, i.e. 2107, 2112, 2603 or 2211.

The Analyzer has a linear response down to 2 Hz, so that the low-frequency limit for correct integration is determined by the input impedance of the integrating networks and the capacity of the accelerometer.

Specifications.

Frequency Response with 2203, using Accelerometer with capacity 1ooo pF.

Velocity.

10 Hz—10 kHz ± 1.5 dB. (20 Hz—10 kHz for 2203 with Serial Number lower than 137745) 25 Hz—5 kHz ± o.5 dB.

Displacement.

20 Hz—4 kHz ± 1.5 dB

50 Hz—2 kHz ± o.5 dB

Temperature Coefficients:

Velocity, + o.02 dB/°C

Displacement, + o.04 dB/°C

The Cathode Follower (2612 or 2613) will heat the Integrator slightly.

AUGUST 1965

Brüel & Kjær

ADR.: BRÜEL & KJÆR
NÆRUM - DENMARK

TELEPHONE: 800500
BRUKJA, Copenhagen

TELEX 5316

PRINT: K. LARSEN & SØN, DENMARK